



# B meson decays to final states containing charmonia at LHCb

Christian Linn, Heidelberg University

On behalf of the LHCb collaboration

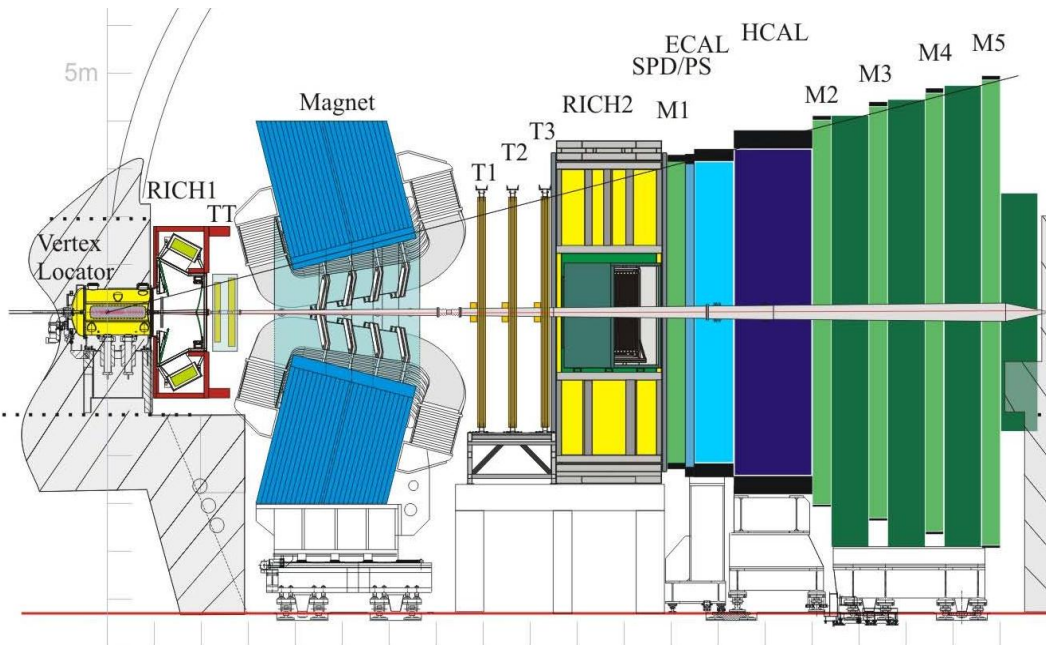




- LHCb detector
- relative branching ratios of  $B \rightarrow \Psi(2s) X$  modes
- Results for  $B_s \rightarrow J/\Psi (h^+ h^-)$  decays important for CPV measurements
  - resonant structure in  $B_s \rightarrow J/\Psi \pi^+ \pi^-$  decays
  - branching ratio of  $B_s \rightarrow J/\Psi K_s (\pi\pi)$
  - angular analysis of  $B_s \rightarrow J/\Psi K^*(K\pi)$
- Summary



# LHCb detector



Advantages of LHCb relevant for  $B \rightarrow J/\Psi X$  decays:

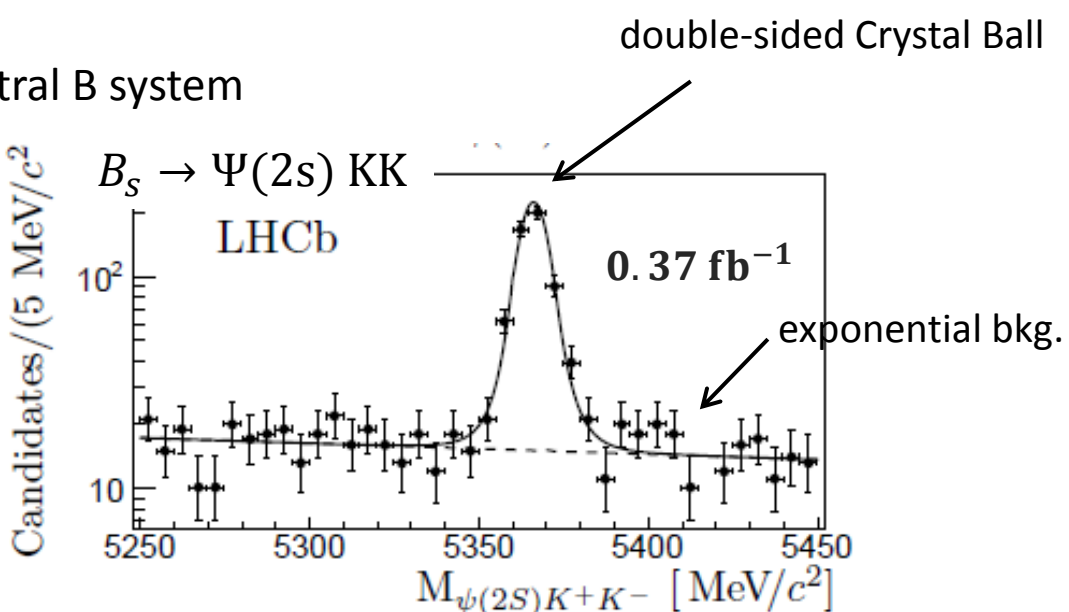
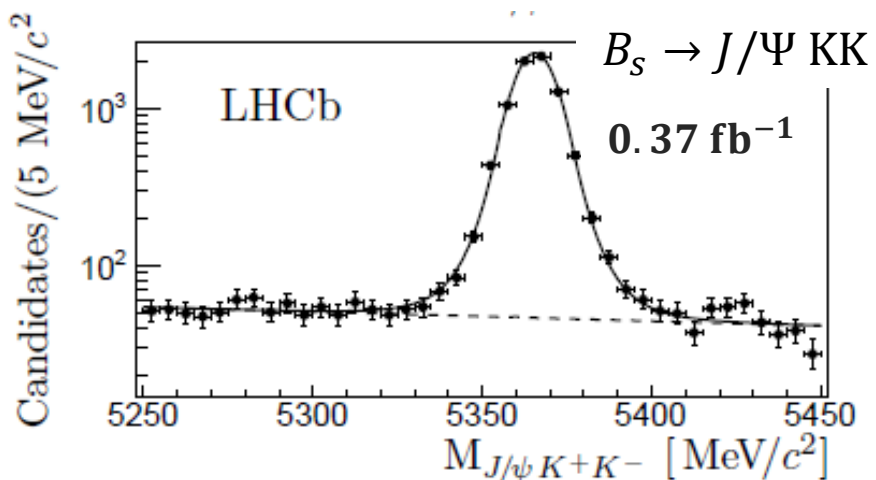
- dedicated single and di-muon trigger with high efficiency
- good time resolution to select B candidates
- good muon identification
- good  $K - \pi$  separation due to RICH detectors



# Relative BR $B \rightarrow \Psi(2s)X$ and $B \rightarrow J/\Psi X$



probe charmonium properties  
explore new channels for CP measurements in neutral B system



- subtraction of non-resonant  $B^0 \rightarrow J/\Psi K\pi$  and  $B_s \rightarrow J/\Psi KK$  contribution
- efficiencies from simulation

Relative branching ratios → most systematic uncertainties cancel:

$$\frac{BR(B^+ \rightarrow \Psi(2s)K^+)}{BR(B^+ \rightarrow J/\Psi K^+)} = 0.594 \pm 0.006 \text{ (stat)} \pm 0.016 \text{ (syst)} \pm 0.015 \text{ (R}_\Psi\text{)}$$

$$\frac{BR(B^0 \rightarrow \Psi(2s)K^*)}{BR(B^0 \rightarrow J/\Psi K^*)} = 0.476 \pm 0.014 \text{ (stat)} \pm 0.010 \text{ (syst)} \pm 0.012 \text{ (R}_\Psi\text{)}$$

$$\frac{BR(B_s^0 \rightarrow \Psi(2s) \Phi)}{BR(B_s^0 \rightarrow J/\Psi \Phi)} = 0.489 \pm 0.026 \text{ (stat)} \pm 0.021 \text{ (syst)} \pm 0.012 \text{ (R}_\Psi\text{)}$$

**main systematics:**  
non-resonant component  
Data – MC agreement

→ significantly more precise than current world average (PDG)



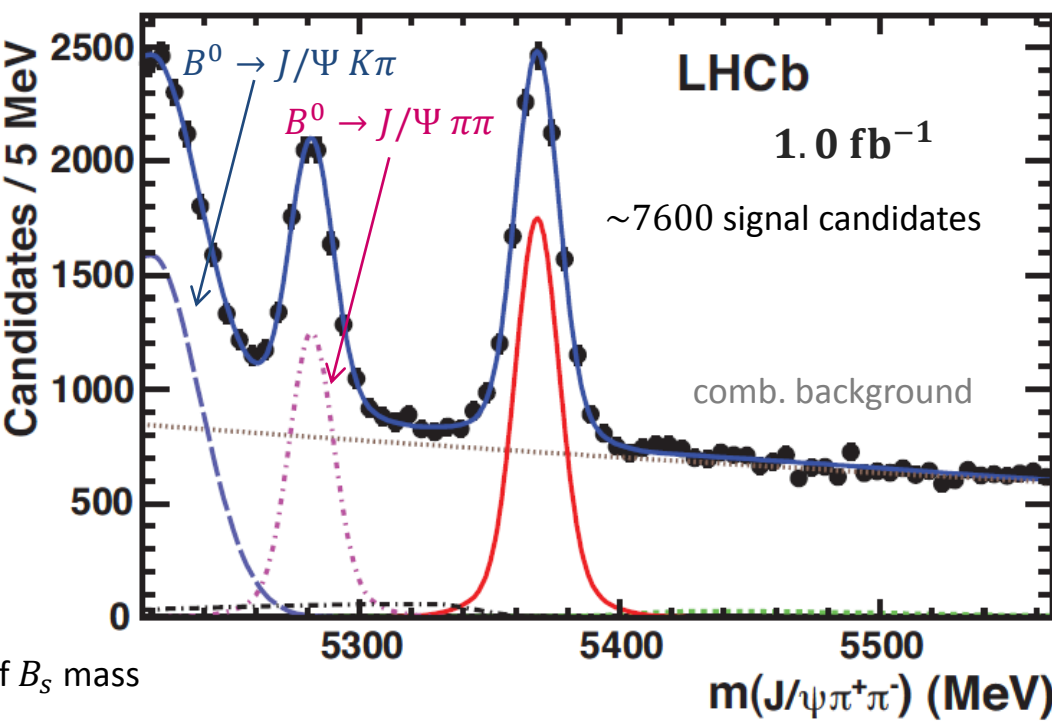
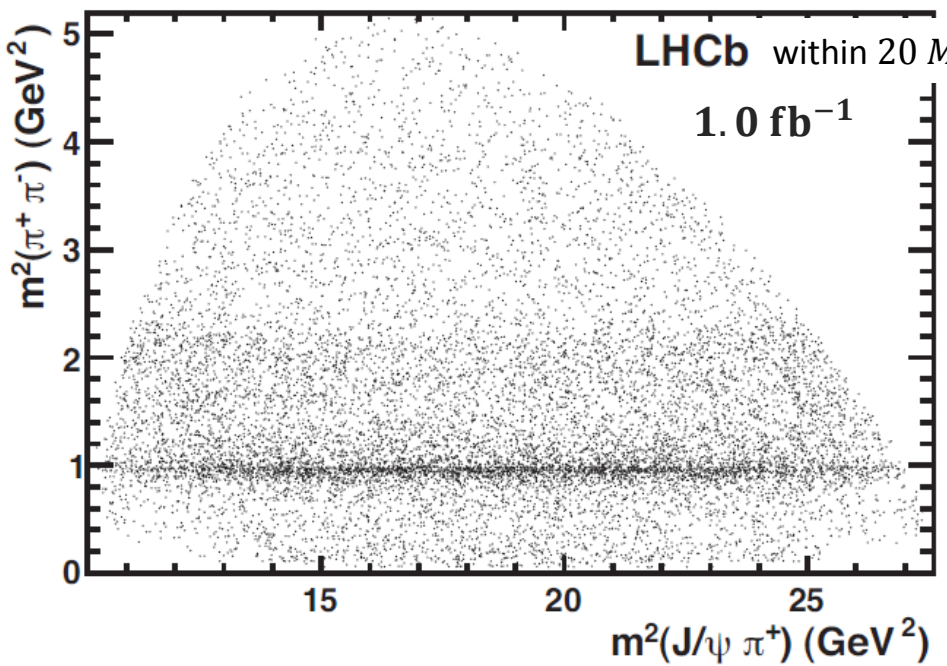
$B_s \rightarrow J/\Psi \pi^+ \pi^-$  decays



➤  $B_s \rightarrow J/\Psi \pi\pi$  decay channels important for measurement of  $B_s - \overline{B}_s$  mixing phase  $\phi_s$  (see talk by G. Cowan)

→ exploit  $\pi\pi$  mass range to determine the resonance structure and CP content

Modified Dalitz plot analysis using  $m^2(J/\Psi \pi^+)$ ,  $m^2(\pi^+\pi^-)$  and helicity angle  $\theta_{J/\Psi}$



- Signal models used in fits:  
sum of interfering  $\pi^+\pi^-$  resonance
- Background shape from wrong-sign  $J/\Psi \pi^\pm \pi^\pm$  events
- Efficiencies from simulation

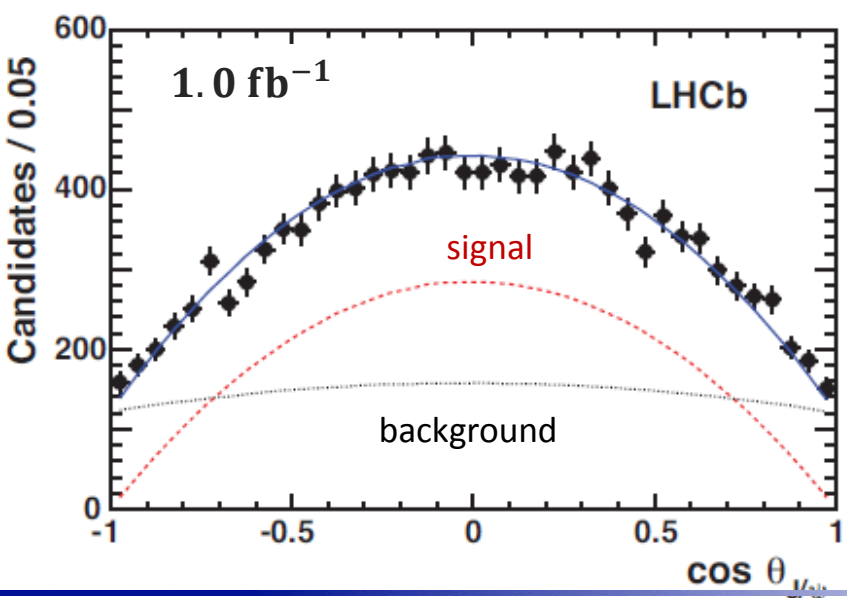
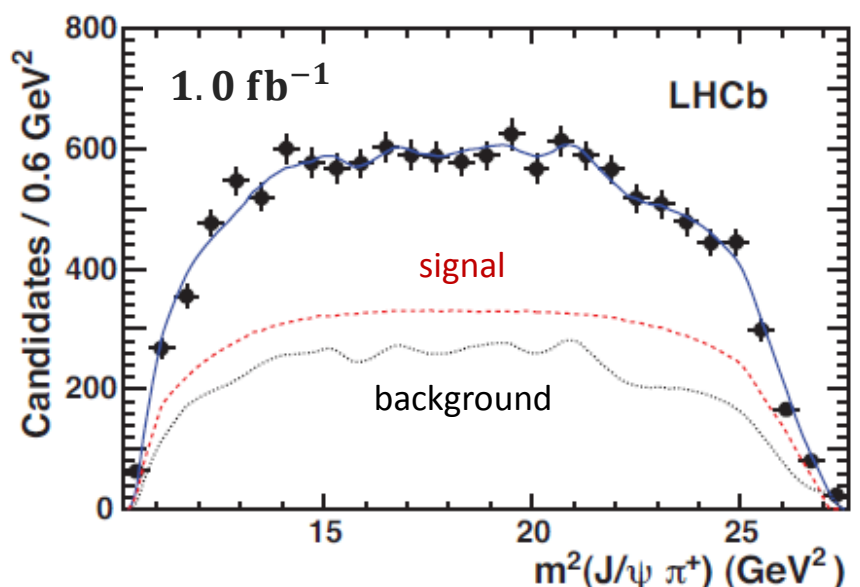
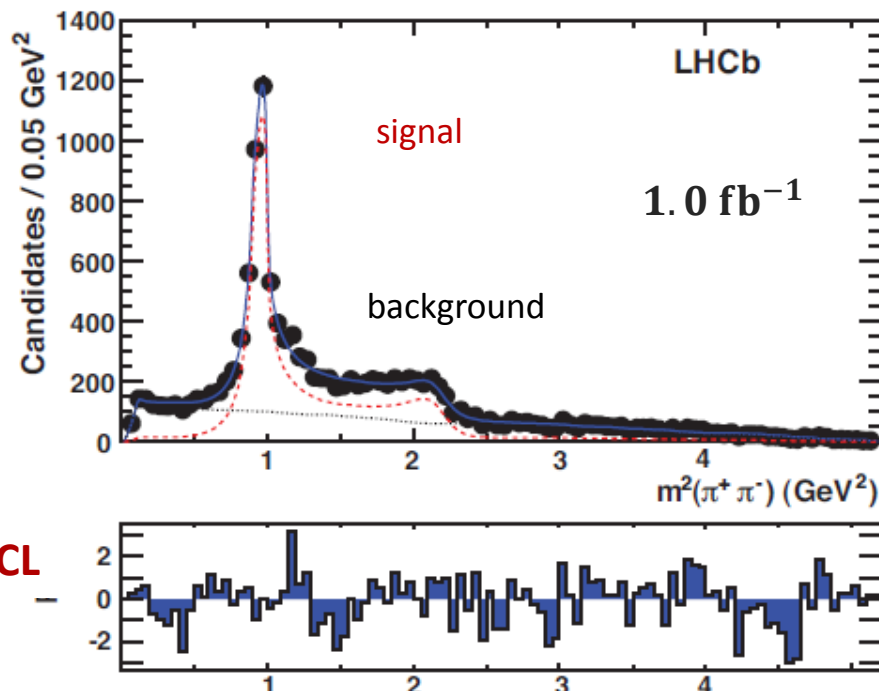


Signal models:

Name	Components
Single R	$f_0(980)$
2R	$f_0(980) + f_0(1370)$
3R	$f_0(980) + f_0(1370) + f_2(1270)$
3R+NR	$f_0(980) + f_0(1370) + f_2(1270) +$ non-resonant
3R+NR + $\rho(770)$	$f_0(980) + f_0(1370) + f_2(1270) +$ non-resonant + $\rho(770)$
3R+NR + $f_0(1500)$	$f_0(980) + f_0(1370) + f_2(1270) +$ non-resonant + $f_0(1500)$
3R+NR + $f_0(600)$	$f_0(980) + f_0(1370) + f_2(1270) +$ non-resonant + $f_0(600)$

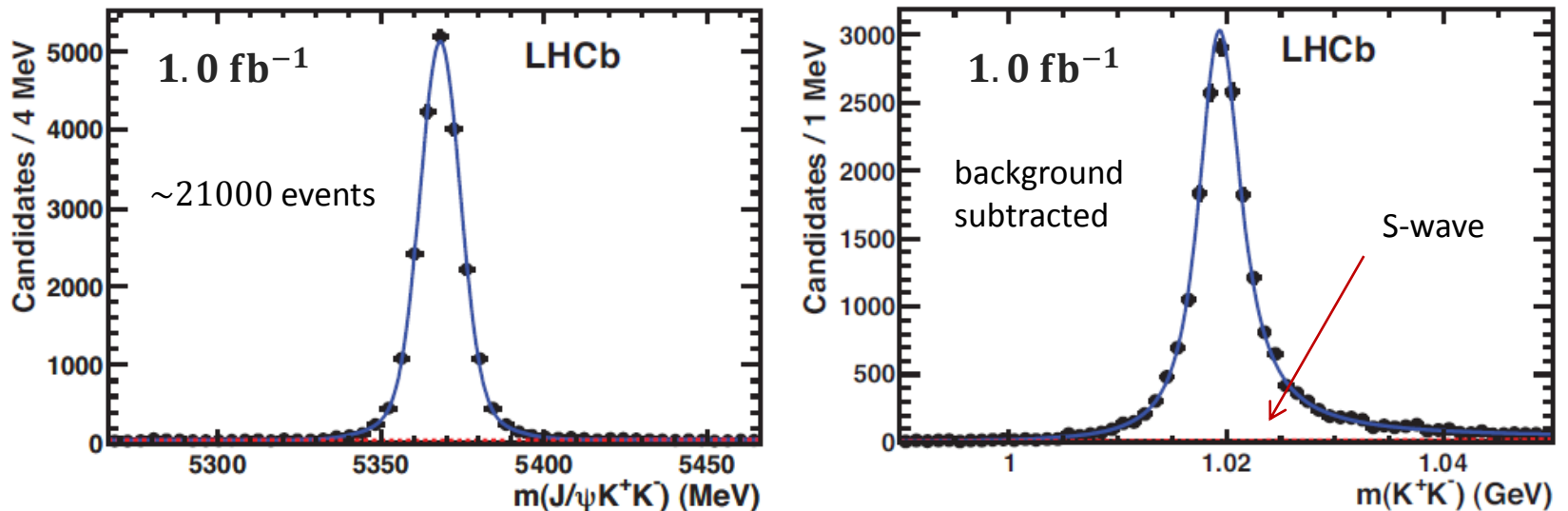
Preferred model gives: smaller than  $3\sigma$  significance

- ~70%  $f_0(980)$
- ~21%  $f_0(1370)$
- ~8.5% non-resonant
- ~0.5%  $f_2(1270)$  helicity 0

**CP-odd fraction > 0.977 at 95%CL**



with  $B_s \rightarrow J/\Psi \Phi$  as normalization channel:



$$\frac{\mathcal{BR}(B_s \rightarrow J/\Psi \pi^+ \pi^-)}{\mathcal{BR}(B_s \rightarrow J/\Psi \Phi)} = (21.28 \pm 0.51 \pm 0.56)\%$$

$$\begin{aligned} f_0(980): & (14.9 \pm 0.6 {}^{+2.8}_{-0.3}) \% \\ f_2(1270): & (0.49 \pm 0.16 {}^{+0.02}_{-0.08}) \% \\ f_0(1370): & (4.51 \pm 0.57 {}^{+0.11}_{-3.30}) \% \end{aligned}$$

Parameter	Total	$f_0(980)$	$f_0(1370)$	NR	$f_2(1270), \lambda = 0$
$m(\pi^+\pi^-)$ dependent eff.	1.0	0.2	0.2	1.0	0.2
PID efficiency	2.0	2.0	2.0	2.0	2.0
$J/\Psi \phi$ S-wave	0.7	0.7	0.7	0.7	0.7
$\bar{B}_s^0$ $p$ and $p_T$ distributions	0.5	0.5	0.5	0.5	0.5
Acceptance function	0	0.1	1.3	1.4	3.9
$\mathcal{B}(\phi \rightarrow K^+K^-)$	1.0	1.0	1.0	1.0	1.0
Background	0.6	0.6	0.6	0.6	0.6
Resonance fit	—	$+18.2$ $-0$	$+0$ $-73.0$	$+34.9$ $-0$	$+0$ $-15.8$
Total	$\pm 2.7$	$+18.3$ $-2.4$	$+2.4$ $-73.0$	$+35.0$ $-3.0$	$+4.6$ $-16.4$

two almost degenerate  
solutions of each fit:  
full difference as syst. error



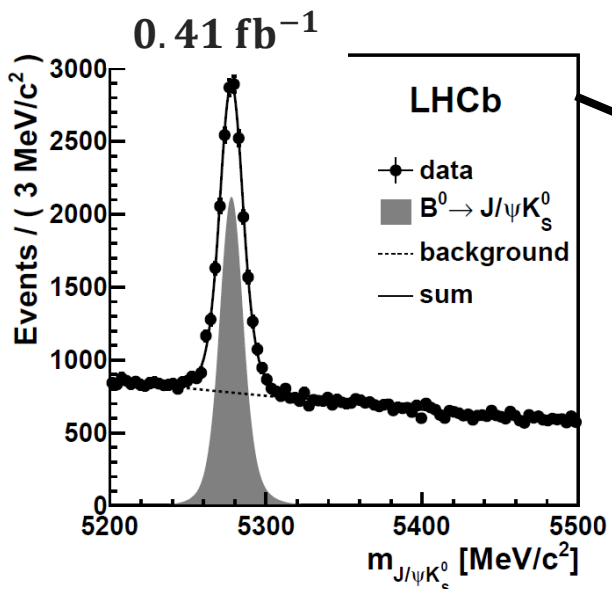
$B_s \rightarrow J/\Psi K_s(\pi\pi)$  and  $B_s \rightarrow J/\Psi K^*(K\pi)$



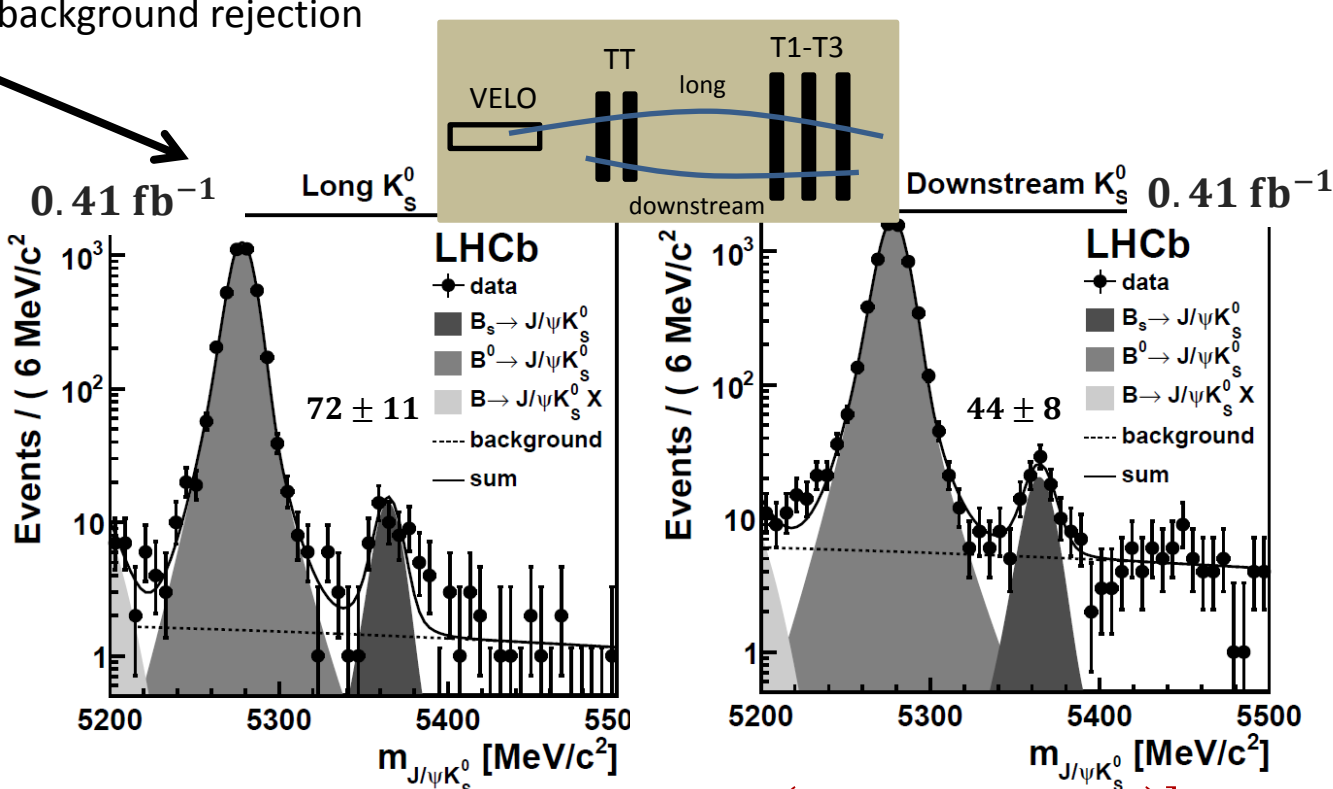
$B_s \rightarrow J/\Psi K_s^0$  is candidate to measure penguin contribution in  $B^0 \rightarrow J/\Psi K_s^0$

(R. Fleischer, Eur. Phys. J. C10 (1999) 299)

here: BR measurement as first step



$B^0$  sample used to train NN  
for background rejection



Main systematics:  
mass shape, geometrical acceptance

$$BR(B_s \rightarrow J/\Psi K_s^0) = [1.83 \pm 0.21 \text{ (stat)} \pm 0.10 \text{ (syst)} \pm 0.14 \text{ } (f_s/f_d) \pm 0.07 \left( BR(B^0 \rightarrow J/\Psi K_s^0) \right)] \cdot 10^{-5}$$

LHCb result: Phys. Rev. Lett. 107 (2011) 211801

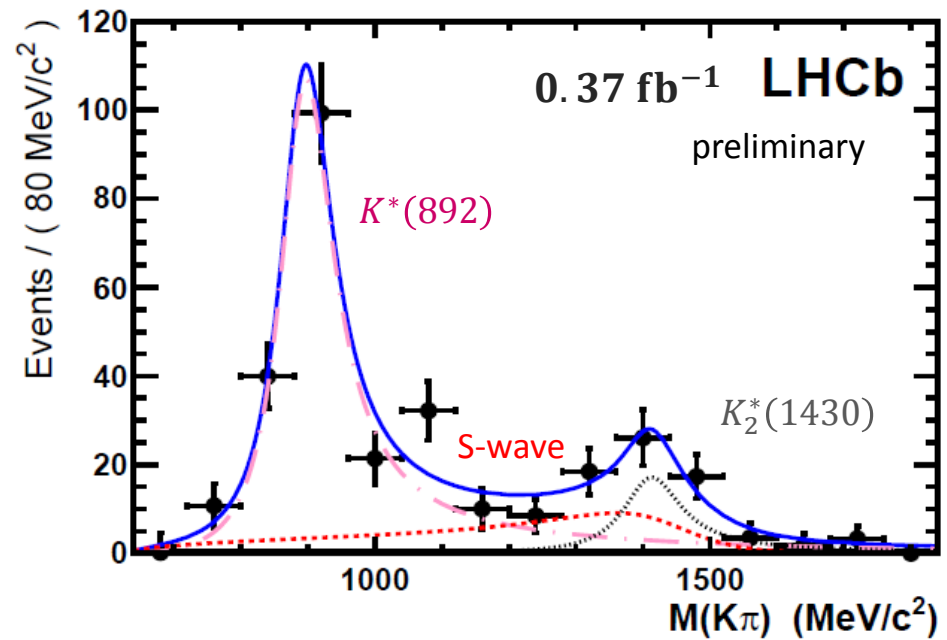
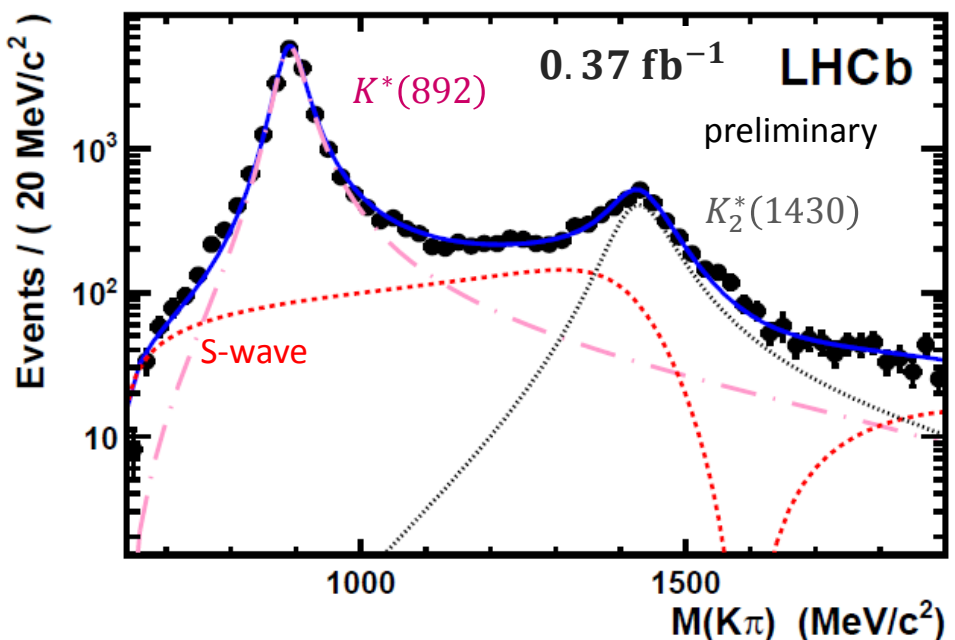
→ most precise measurement to date and compatible with expectations from  $SU(3)$



- $B_s \rightarrow J/\Psi K^*$  gives possibility to control penguin contribution in  $B_s \rightarrow J/\Psi \Phi$   
(Faller, Fleischer, Mannel, Phys. Rev. D79 (2009) 014005 )
- already preliminary LHCb branching ratio measurement
- Now: improved branching ratio measurement, **study angular properties**

### $B^0 \rightarrow J/\Psi K^*$ as normalization channel

Mass fit including: S-wave, P-wave ( $K^*$ ) , D-wave ( $K_2^*(1430)$ ), F-wave ( $K_3^*(1780)$ ), H-wave ( $K_4^*(2045)$ )

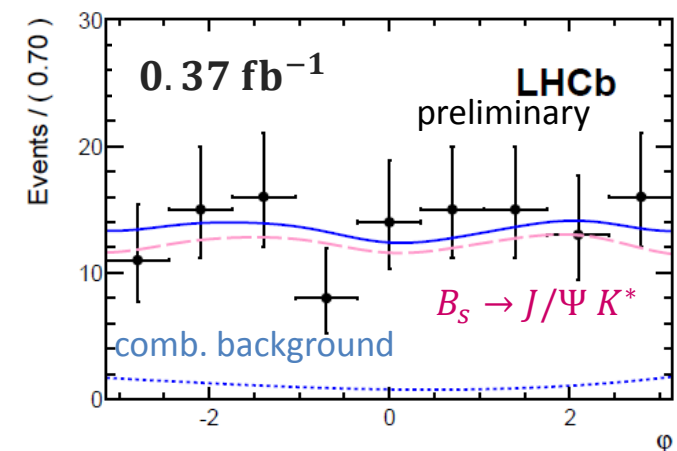
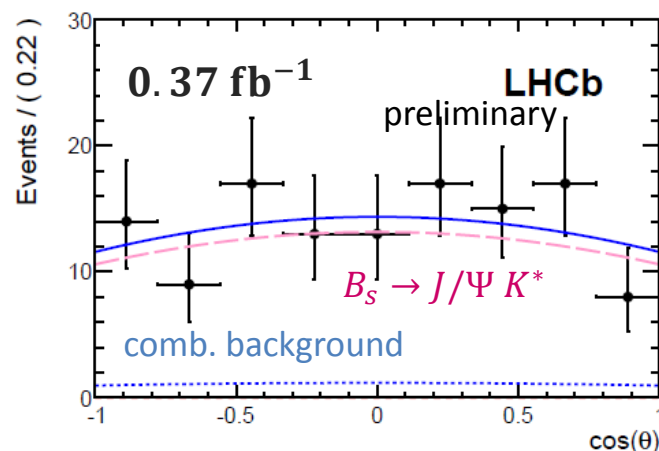
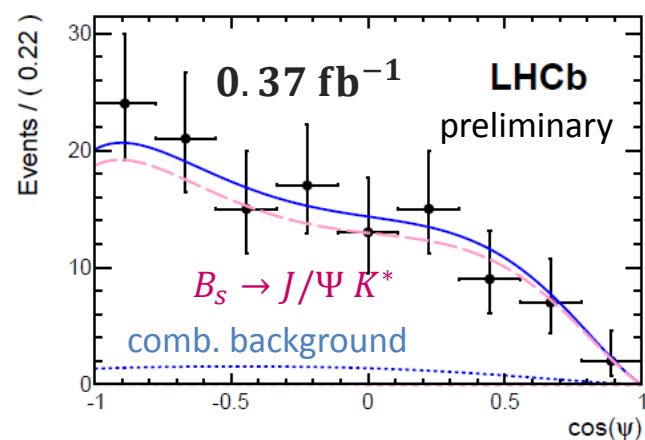
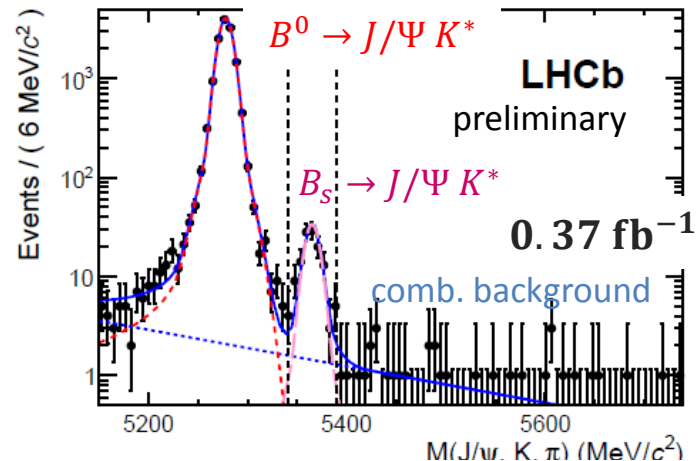


$\pm 40$  MeV around  $K^*$  mass  $\rightarrow f_{K^*}^{B^0} = 97\%$

$f_{K^*}^{B_s} = 96\%$



- Simultaneous fit of mass and angular distributions of  $B_s$  and  $B^0$
- fit includes also non-resonant contributions
- $B^0 \rightarrow J/\Psi K^*$  polarization fractions as cross-check



Fraction of longitudinal polarized vector mesons:

$$f_L = 0.503^{+0.075}_{-0.078} \text{ (stat)} \pm 0.021 \text{ (syst)} \quad (\text{preliminary})$$

Fraction of transversely, parallel polarized vector mesons:

$$f_{\parallel} = 0.187^{+0.099}_{-0.080} \text{ (stat)} \pm 0.022 \text{ (syst)} \quad (\text{preliminary})$$

→ first measurement of polarization fractions in  $B_s \rightarrow J/\Psi K^*(892)$

$$BR(B_s \rightarrow J\Psi K^*) = \left( 4.42^{+0.46}_{-0.44} \text{ (stat)} \pm 0.80 \text{ (syst)} \right) \cdot 10^{-5} \quad (\text{preliminary})$$

Main systematics:  
angular acceptance, bkg model



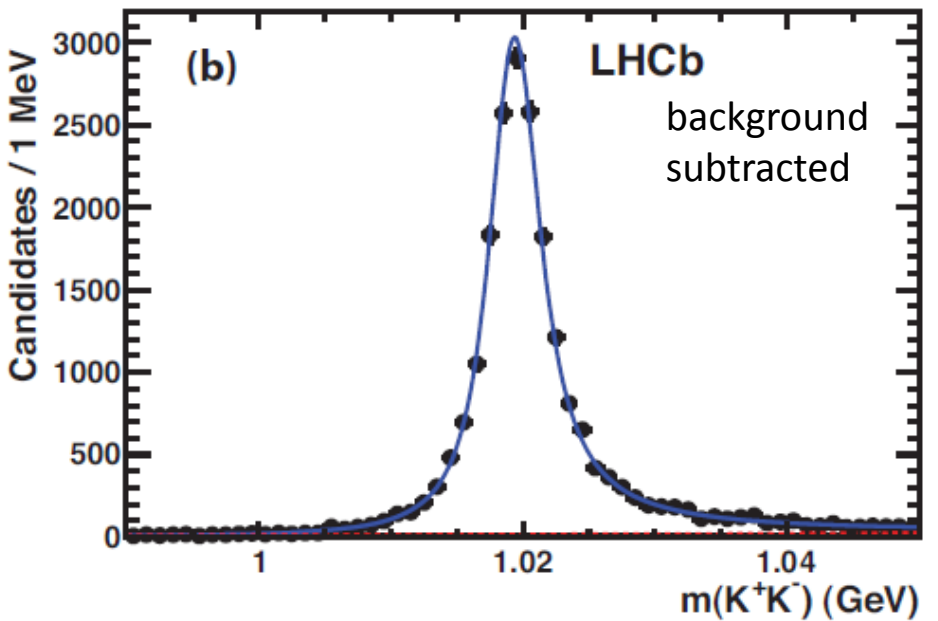
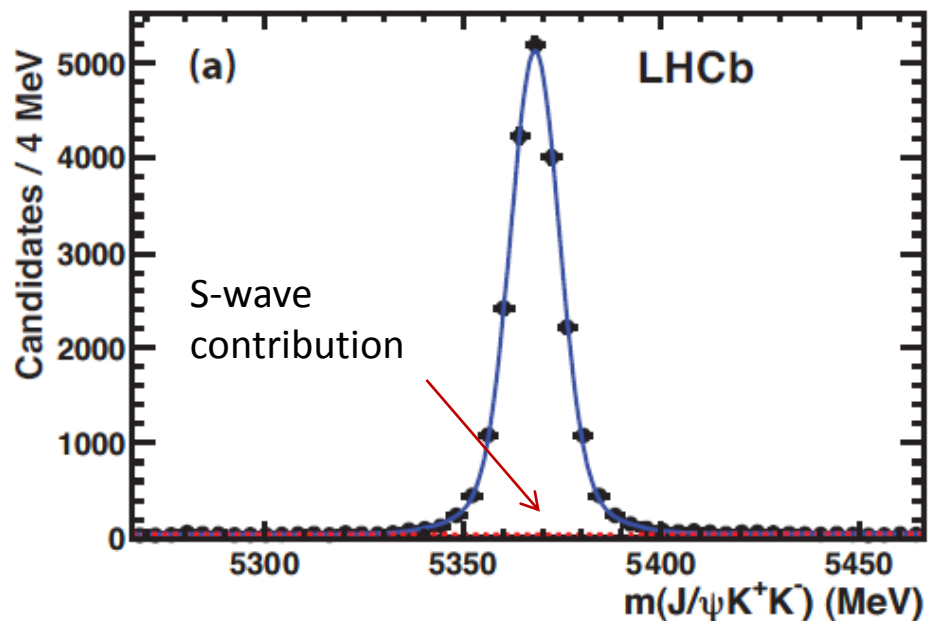
- LHCb shows excellent performance in measuring B decays to charmonia
- First investigation of resonance structure in  $B_s \rightarrow J/\Psi \pi\pi$  decays  
→ provides new data sample for  $\phi_s$  measurement (see talk by G. Cowan)
- most precise branching ratio measurement of  $B_s \rightarrow J/\Psi K_s$
- first measurement of polarization fractions of  $B_s \rightarrow J/\Psi K^*$
- LHCb has already collected  $\sim 600 \text{ pb}^{-1}$  in 2012 ( still ongoing )  
→ more results to come...



# Backup

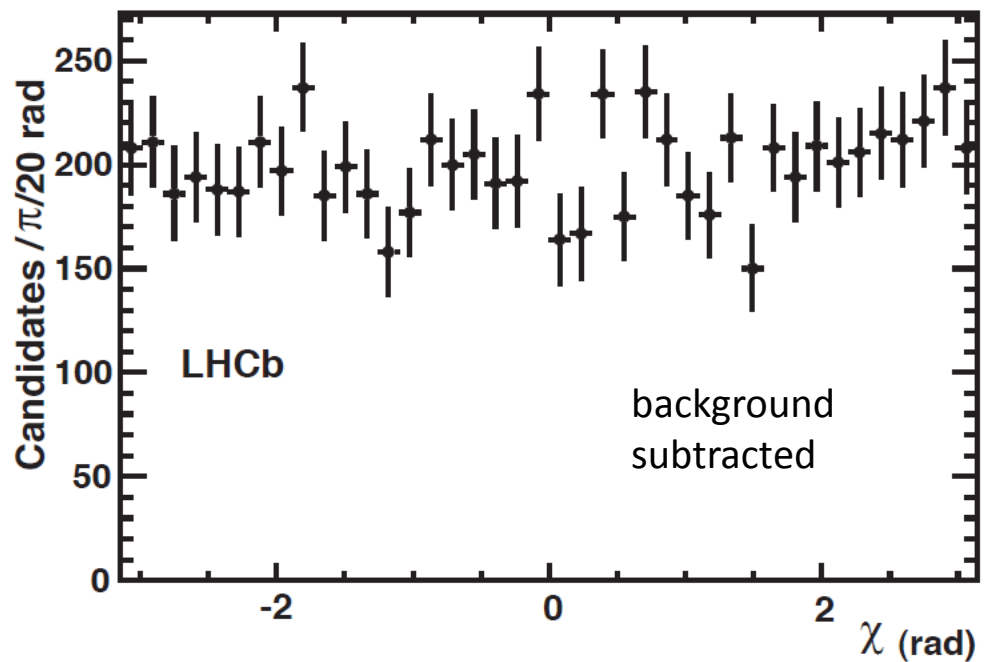


Invariant mass spectra of  $B_s \rightarrow J/\Psi \Phi(KK)$  events (used as normalization channel for BR measurement)



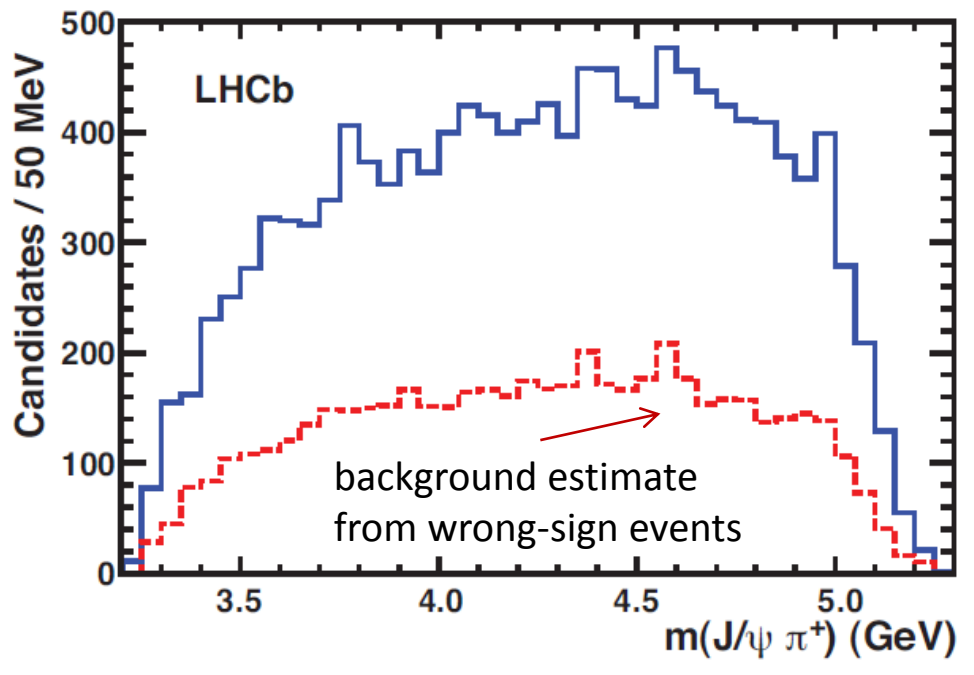


$\chi$  (angle between  $J/\Psi$  and  $\pi\pi$  decay plane) distribution:



No structure  $\rightarrow$  integrated over  $\chi$  in analysis procedure

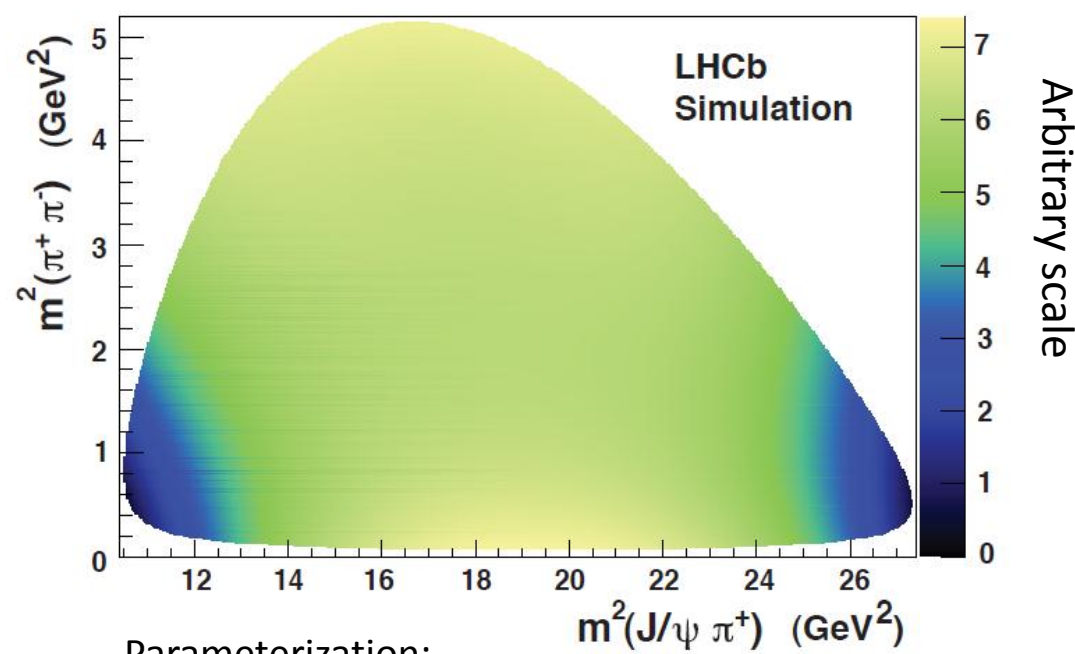
$m(J/\Psi \pi)$  distribution for  $m_B \pm 20\text{MeV}$ :



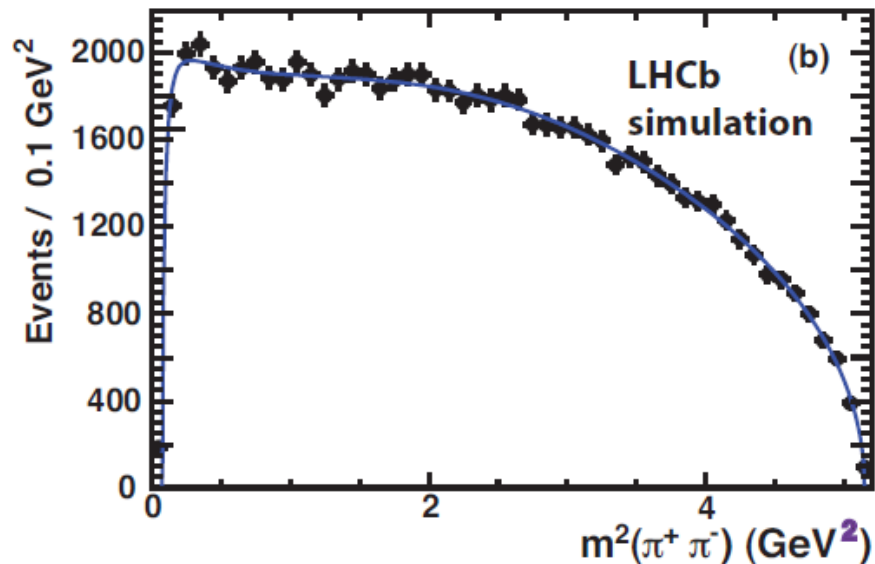
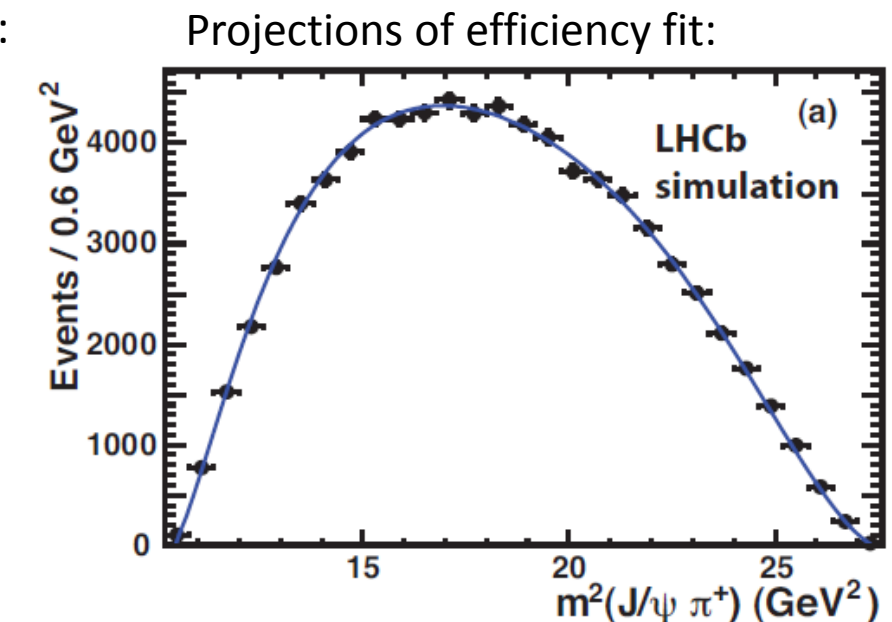
No visible structure



Detection efficiency determined from  $B_s \rightarrow J/\Psi \pi\pi$  MC:



Parameterization:  
symmetric 4th order polynomial function





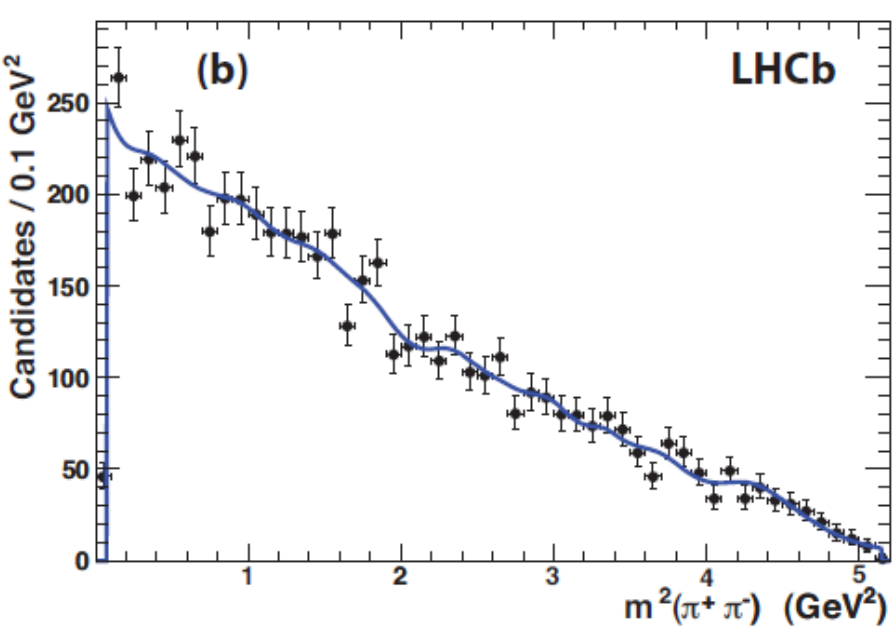
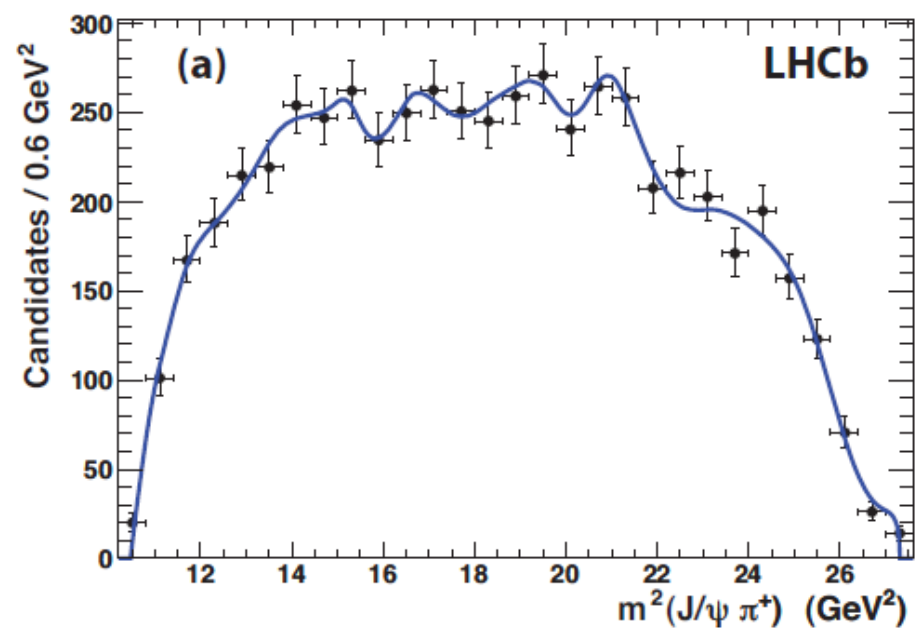
Background composition:

Wrong-sign events in  $m_B \pm 20\text{MeV}$

4.5% contribution of combinatoric

$J/\Psi + \text{random } \rho(770)$  from MC

### Projections of background fit





Resonance models used in fit:

	Resonance	Spin	Helicity	Resonance formalism
	$f_0(600)$	0	0	BW
	$\rho(770)$	1	$0, \pm 1$	BW
	$f_0(980)$	0	0	Flatté
	$f_2(1270)$	2	$0, \pm 1$	BW
	$f_0(1370)$	0	0	BW
	$f_0(1500)$	0	0	BW

Table 3: Breit-Wigner resonance parameters.

Resonance	Mass (MeV)	Width (MeV)	Source	
$f_0(600)$	$513 \pm 32$	$335 \pm 67$	CLEO [20]	
$\rho(770)$	$775.5 \pm 0.3$	$149.1 \pm 0.8$	PDG [8]	
$f_2(1270)$	$1275 \pm 1$	$185 \pm 3$	PDG [8]	
$f_0(1370)$	$1434 \pm 20$	$172 \pm 33$	E791 [21]	← not fixed in fit
$f_0(1500)$	$1505 \pm 6$	$109 \pm 7$	PDG [8]	

Maximum likelihood fit to determine the complex amplitudes:

One magnitude and one phase in each helicity group are fixed:  $f_0(980)$  and  $f_2(1270)$  with helicity  $\pm 1$

All background and efficiency parameters fixed



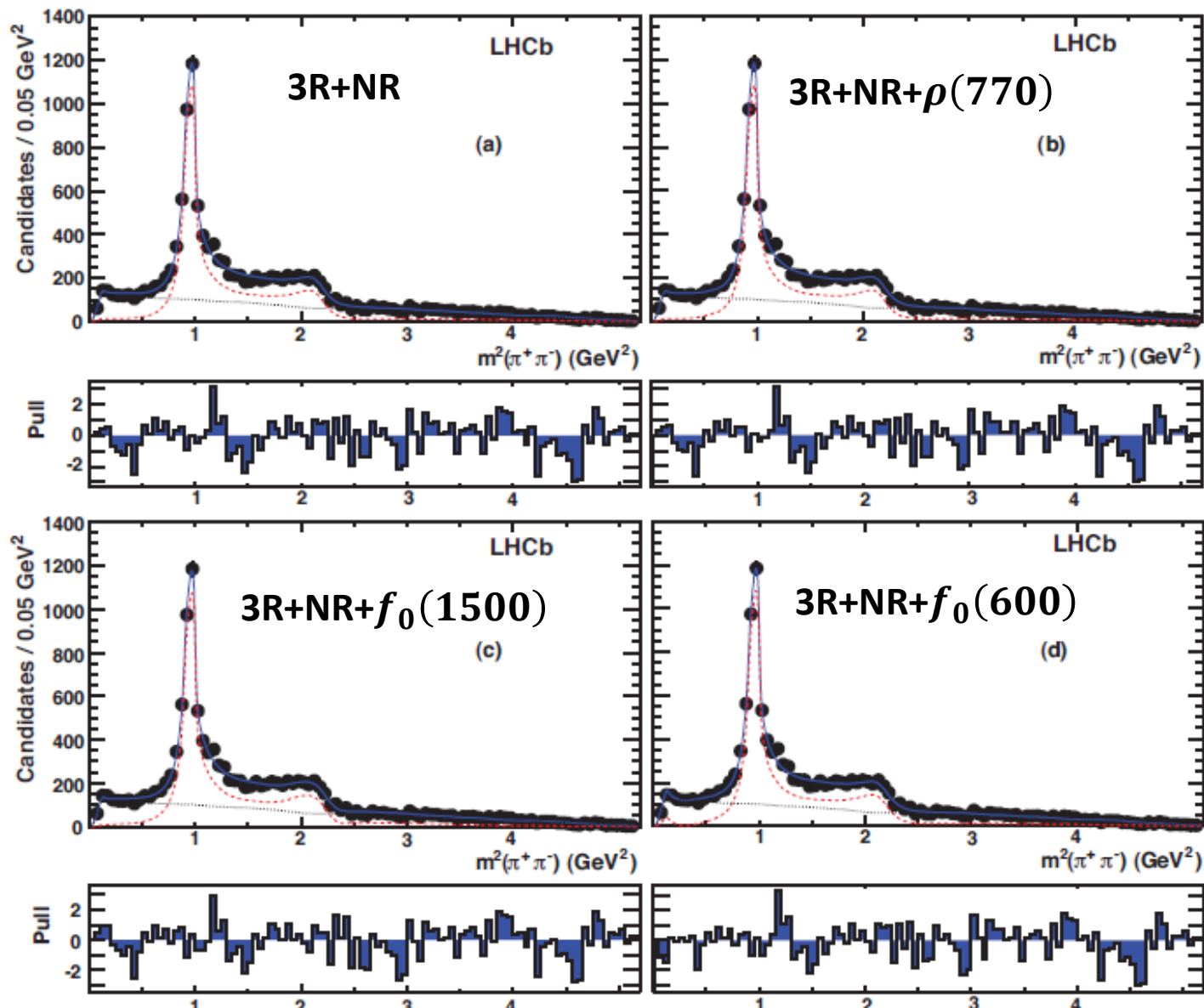
Fit results:

Table 4:  $\chi^2/\text{ndf}$  and  $-\ln\mathcal{L}$  of different resonance models.

Resonance model	$-\ln\mathcal{L}$	$\chi^2/\text{ndf}$	Probability (%)
Single R	59269	1956/1352	0
2R	59001	1498/1348	0.25
3R	58973	1455/1345	1.88
3R+NR (preferred)	58945	1415/1343	8.41
3R+NR (alternate)	58946	1414/1343	8.70
3R+NR + $\rho(770)$ (preferred)	58945	1418/1341	7.05
3R+NR + $\rho(770)$ (alternate)	58944	1416/1341	7.57
3R+NR + $f_0(1500)$ (preferred)	58943	1416/1341	7.57
3R+NR + $f_0(1500)$ (alternate)	58941	1407/1341	10.26
3R+NR + $f_0(600)$ (preferred)	58935	1409/1341	9.60
3R+NR + $f_0(600)$ (alternate)	58937	1412/1341	8.69



Fit projections:





Fit fractions:

Components	3R+NR	3R+NR+ $\rho$	3R+NR+ $f_0(1500)$	3R+NR+ $f_0(600)$
$f_0(980)$	$107.09 \pm 3.51$	$104.84 \pm 3.91$	$72.99 \pm 5.82$	$115.24 \pm 5.32$
$f_0(1370)$	$32.57 \pm 4.10$	$32.30 \pm 3.72$	$113.67 \pm 13.57$	$34.47 \pm 3.98$
$f_0(1500)$	-	-	$15.00 \pm 4.83$	-
$f_0(600)$	-	-	-	$4.68 \pm 2.46$
NR	$12.84 \pm 2.32$	$12.16 \pm 2.22$	$10.66 \pm 2.06$	$23.65 \pm 3.59$
$f_2(1270), \lambda = 0$	$0.76 \pm 0.25$	$0.77 \pm 0.25$	$1.07 \pm 0.37$	$0.90 \pm 0.31$
$f_2(1270),  \lambda  = 1$	$0.33 \pm 1.00$	$0.26 \pm 1.12$	$1.02 \pm 0.83$	$0.61 \pm 0.87$
$\rho, \lambda = 0$	-	$0.66 \pm 0.53$	-	-
$\rho,  \lambda  = 1$	-	$0.11 \pm 0.78$	-	-
Sum	$153.6 \pm 6.0$	$151.1 \pm 6.0$	$214.4 \pm 15.7$	$179.6 \pm 8.0$
$-\ln \mathcal{L}$	58945	58944	58943	58935
$\chi^2/\text{ndf}$	1415/1343	1418/1341	1416/1341	1409/1341
Probability(%)	8.41	7.05	7.57	9.61

Components	3R+NR	3R+NR+ $\rho$	3R+NR+ $f_0(1500)$	3R+NR+ $f_0(600)$
$f_0(980)$	$100.81 \pm 2.87$	$99.15 \pm 4.20$	$96.89 \pm 3.82$	$110.70 \pm 14.76$
$f_0(1370)$	$7.00 \pm 0.91$	$6.93 \pm 0.93$	$2.99 \pm 1.68$	$7.99 \pm 1.06$
$f_0(1500)$	-	-	$4.68 \pm 1.73$	-
$f_0(600)$	-	-	-	$4.29 \pm 2.26$
NR	$13.80 \pm 2.32$	$13.42 \pm 2.67$	$13.35 \pm 2.39$	$24.71 \pm 3.91$
$f_2(1270), \lambda = 0$	$0.51 \pm 0.14$	$0.52 \pm 0.14$	$0.50 \pm 0.14$	$0.51 \pm 0.14$
$f_2(1270),  \lambda  = 1$	$0.24 \pm 1.11$	$0.19 \pm 1.38$	$0.63 \pm 0.84$	$0.48 \pm 0.89$
$\rho, \lambda = 0$	-	$0.43 \pm 0.55$	-	-
$\rho,  \lambda  = 1$	-	$0.14 \pm 0.78$	-	-
Sum	$122.4 \pm 4.0$	$120.8 \pm 5.3$	$119.2 \pm 5.2$	$148.7 \pm 15.5$
$-\ln \mathcal{L}$	58946	58945	58941	58937
$\chi^2/\text{ndf}$	1414/1343	1416/1341	1407/1341	1412/1341
Probability(%)	8.70	7.57	10.26	8.69



Fit fractions of interference terms for 3R+NR:

Components	Preferred	Alternate
$f_0(980) + f_0(1370)$	$-36.6 \pm 4.6$	$-5.4 \pm 2.3$
$f_0(980) + \text{NR}$	$-16.1 \pm 2.7$	$-23.6 \pm 2.6$
$f_0(1370) + \text{NR}$	$0.8 \pm 1.0$	$6.6 \pm 0.8$
Sum	$-53.6 \pm 5.5$	$-22.4 \pm 3.6$

Fit results for 3R+NR:

The parameters	Preferred	Alternate
$m_{f_0(980)}$ (MeV)	$939.9 \pm 6.3$	$939.2 \pm 6.5$
$g_{\pi\pi}$ (MeV)	$199 \pm 30$	$197 \pm 25$
$g_{KK}/g_{\pi\pi}$	$3.0 \pm 0.3$	$3.1 \pm 0.2$
$m_{f_0(1370)}$ (MeV)	$1475.1 \pm 6.3$	$1474.4 \pm 6.0$
$\Gamma_{f_0(1370)}$ (MeV)	$113 \pm 11$	$108 \pm 11$
$\phi_{980}$	0 (fixed)	0 (fixed)
$\phi_{1370}$	$241.5 \pm 6.3$	$181.7 \pm 8.4$
$\phi_{\text{NR}}$	$217.0 \pm 3.7$	$232.2 \pm 3.7$
$\phi_{1270}, \lambda = 0$	$165 \pm 15$	$118 \pm 15$
$\phi_{1270},  \lambda  = 1$	0 (fixed)	0 (fixed)

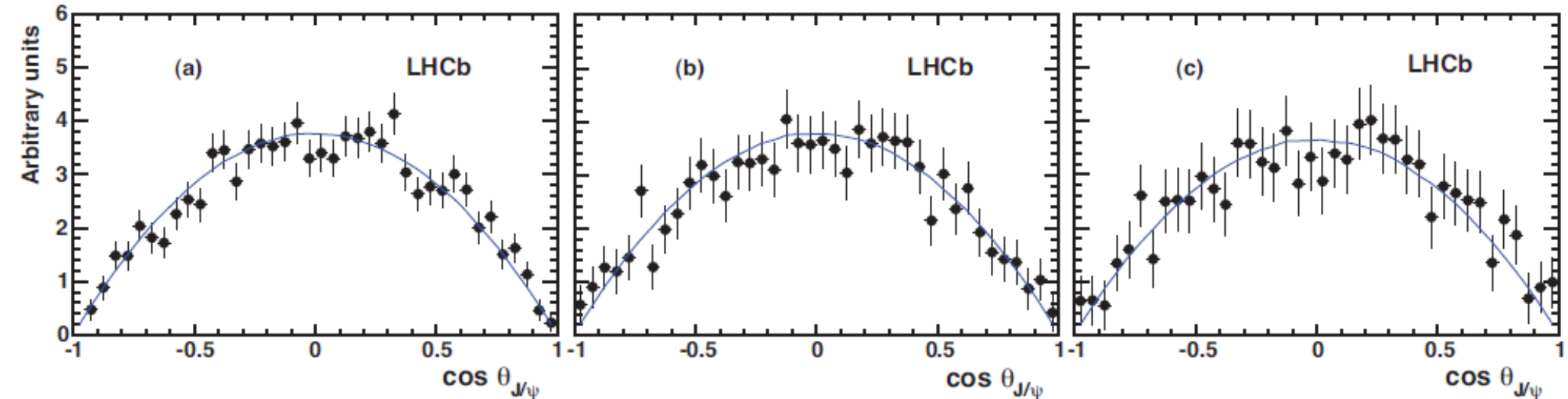


Helicity distributions for preferred model:

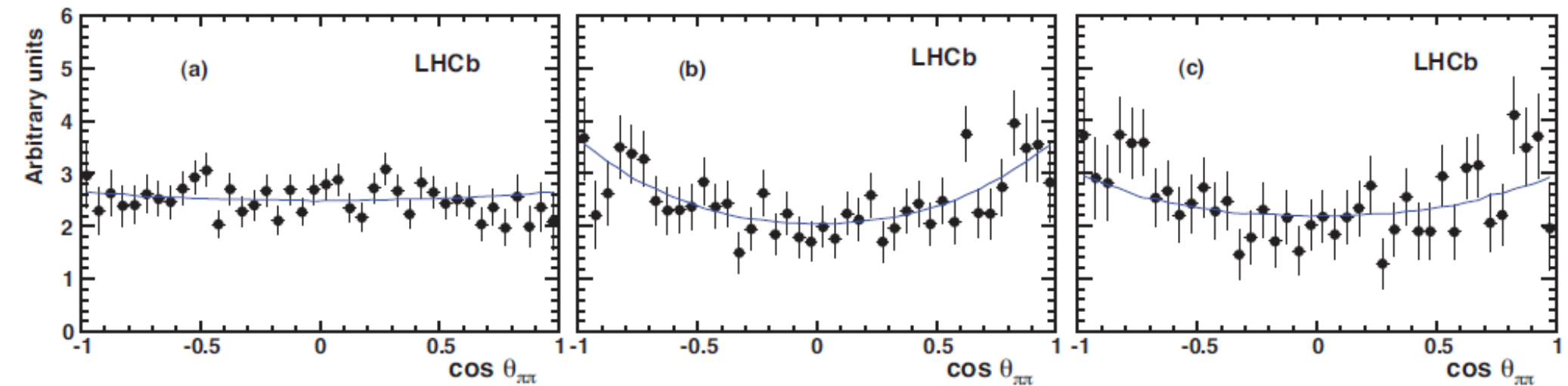
$$f_0(980) \pm 90 \text{ MeV}$$

$$f_2(1270) \pm 185 \text{ MeV}$$

$$f_0(1370) \pm 172 \text{ MeV}$$



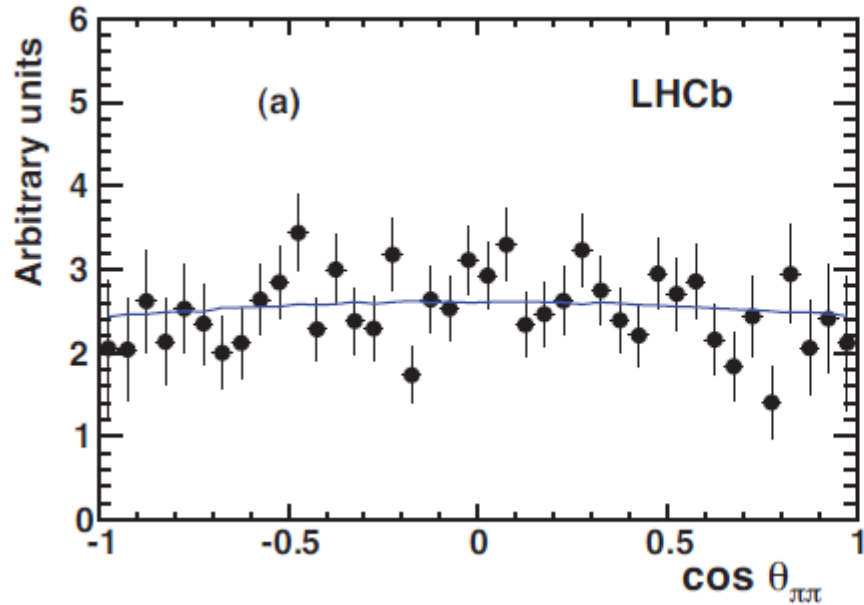
Non-flat  $\cos \theta_{\pi\pi}$  distributions show interference between S-wave and D-wave amplitudes:



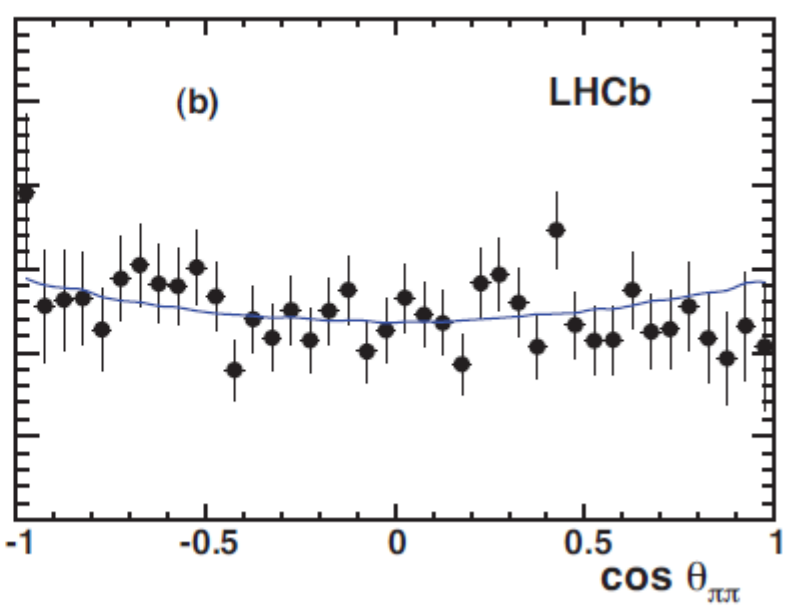


Helicity distributions for preferred model:

$f_0(980) - 90MeV$



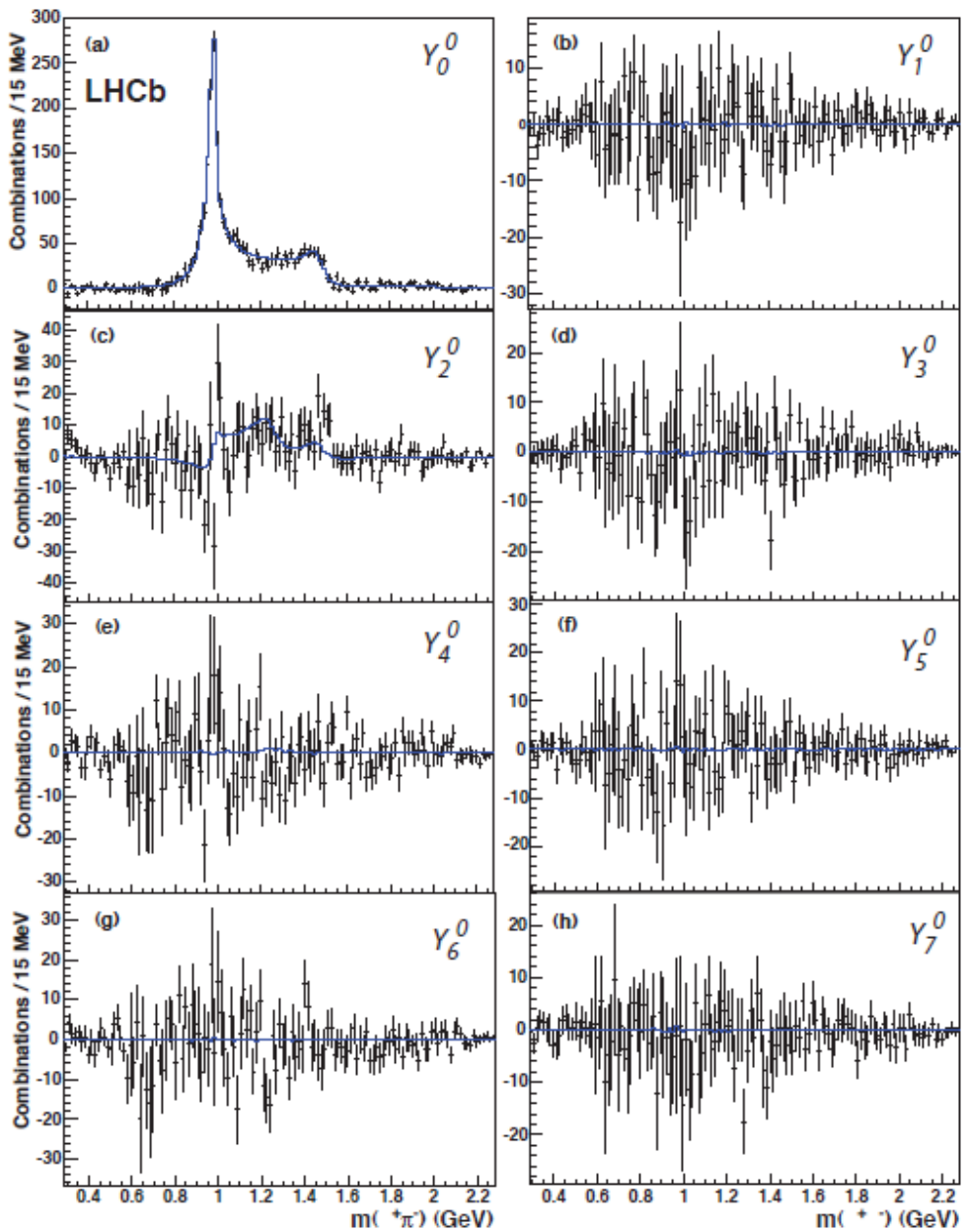
$f_0(980) + 90MeV$



Different shapes due to  $f_0(980)$  phase change by  $\pi$

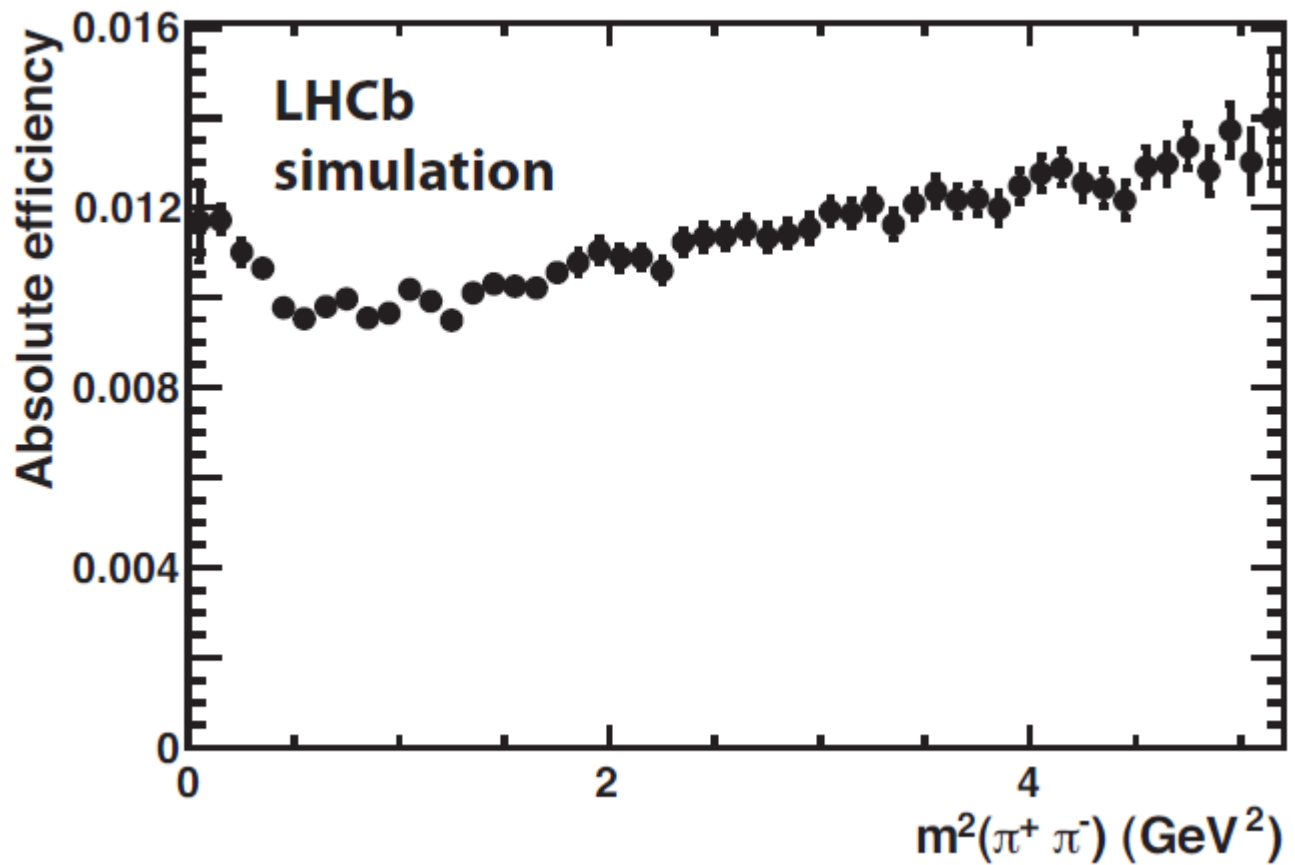


Angular moments of preferred 3R+NR model:





Detection efficiency for BR measurement ( from simulation ):





Systematic uncertainties:

Table 10: Relative systematic uncertainties on  $R$  (%).

Parameter	Total	$f_0(980)$	$f_0(1370)$	NR	$f_2(1270), \lambda = 0$
$m(\pi^+\pi^-)$ dependent eff.	1.0	0.2	0.2	1.0	0.2
PID efficiency	2.0	2.0	2.0	2.0	2.0
$J/\psi\phi$ S-wave	0.7	0.7	0.7	0.7	0.7
$\bar{B}_s^0 p$ and $p_T$ distributions	0.5	0.5	0.5	0.5	0.5
Acceptance function	0	0.1	1.3	1.4	3.9
$\mathcal{B}(\phi \rightarrow K^+K^-)$	1.0	1.0	1.0	1.0	1.0
Background	0.6	0.6	0.6	0.6	0.6
Resonance fit	—	+18.2 -0	+0 -73.0	+34.9 -0	+0 -15.8
Total	$\pm 2.7$	+18.3 -2.4	+ 2.4 -73.0	+35.0 - 3.0	+ 4.6 -16.4

Table 11: Changes due to modified acceptance function.

Values	Original	After change	Variation(%)
Fit fractions			
$f_0(980)$	(107.09±3.51)%	107.19%	0.09
$f_2(1270) \lambda = 0$	(0.76±0.25)%	0.79%	3.9
$f_2(1270)  \lambda  = 1$	(0.33±1.00)%	0.26%	21.2
$f_0(1370)$	(32.57±4.10)%	31.16%	1.3
NR	(12.84±2.32)%	12.66%	1.4
$f_0(980)$ parameters			
$m_{f_0}$ (MeV)	939.9±6.3	938.4	0.16
$g_{\pi\pi}$ (MeV)	199±30	205	2.7
$g_{KK}/g_{\pi\pi}$	3.01±0.25	3.05	1.3
$f_0(1370)$ parameters			
$m_{f_0}$ (MeV)	1475.1±6.3	1476.4	0.09
$\Gamma$ (MeV)	112.7±11.1	113.0	0.27



Measured event yields for  $B^0 \rightarrow J/\Psi K_s$  and  $B_s \rightarrow J/\Psi K_s$ :

	downstream $K_s^0$	long $K_s^0$
$B^0$ in normalisation sample	$1502 \pm 39$	$970 \pm 31$
$B^0$ in normalisation sample (scaled to full)	$6007 \pm 157$	$3879 \pm 124$
$B_s^0$ in full sample	$72 \pm 11$	$44 \pm 8$
Ratio of $B_s^0$ to $B^0$	$0.0120 \pm 0.0018$	$0.0112 \pm 0.0020$
Ratio of $B_s^0$ to $B^0$ (weighted average, $r$ )	$0.0117 \pm 0.0014$	

Correction factors and systematic uncertainties for BR measurement:

Source	Correction factor
Geometrical acceptance ( $\epsilon_{\text{geom}}$ )	$0.987 \pm 0.018$
Trigger and reconstruction	$1.000 \pm 0.010$
Decay time acceptance ( $\epsilon_{\text{time}}$ )	$0.975 \pm 0.007$
Mass shape	$1.000 \pm 0.050$
$B_s^0$ - $B^0$ mass difference	$1.000 \pm 0.004$
Total	$0.962 \pm 0.053$



Comparison with  $SU(3)$  expectations:

$$BR(B_s \rightarrow f)_{theo} = \frac{\tau_{B_s}}{2} (\Gamma(B_s \rightarrow f) + \Gamma(\overline{B_s} \rightarrow f)) \Big|_{t=0} \quad \text{BR definition in theoretical predictions}$$

$$\frac{1-y_s^2}{1+A_{\Delta\Gamma}^{J/\Psi K_s} y_s} = 0.936 \pm 0.015 \quad \text{Correction factor to compare measurement with theoretical prediction}$$

$$y_s = \frac{\Delta\Gamma}{2\Gamma} = 0.075 \pm 0.010 \quad \text{K. De Bruyn et al., arXiv:1204.1735}$$

$$A_{\Delta\Gamma}^{J/\Psi K_s} = 0.84 \pm 0.18 \quad \text{HFAG, arXiv:1010.1589}$$

$$BR(B_s \rightarrow J/\Psi \overline{K^0}) = [3.42 \pm 0.40 \text{ (stat)} \pm 0.19 \text{ (syst)} \pm 0.27 (f_s/f_d) \pm 0.13 (BR(B^0 \rightarrow J/\Psi K^0)) \pm 0.05 (y, A_{\Delta\Gamma})] \cdot 10^{-5}$$

$SU(3)$  symmetry implies equality of  $B_s \rightarrow J/\Psi \bar{K}$  and  $B^0 \rightarrow J/\Psi \pi^0$  decay widths:

From measurement:  $\Xi_{SU(3)} = 0.98 \pm 0.18$



Differential decay rate:

$$\begin{aligned}\frac{d^3\Gamma}{d\Omega} \propto & 2|A_0|^2 \cos^2 \psi (1 - \sin^2 \theta \cos^2 \varphi) \\ & + |A_{||}|^2 \sin^2 \psi (1 - \sin^2 \theta \sin^2 \varphi) \\ & + |A_{\perp}|^2 \sin^2 \psi \sin^2 \theta \\ & + \frac{1}{\sqrt{2}} |A_0| |A_{||}| \cos(\delta_{||} - \delta_0) \sin 2\psi \\ & + \frac{2}{3} |A_S|^2 [1 - \sin^2 \theta \cos^2 \varphi] \\ & + \frac{4\sqrt{3}}{3} |A_0| |A_S| \cos(\delta_S - \delta_0) \cos \psi [1 - \sin^2 \theta \cos^2 \varphi] \\ & + \frac{\sqrt{6}}{3} |A_{||}| |A_S| \cos(\delta_{||} - \delta_S) \sin \psi \sin^2 \theta \sin 2\varphi,\end{aligned}$$



Fit results and systematic uncertainties:

Parameter name	$ A_S _{B_s^0}^2$	$f_L^{B_s^0}$	$f_{\parallel}^{B_s^0}$
Value	$0.072^{+0.15}_{-0.071}$	$0.503^{+0.075}_{-0.078}$	$0.187^{+0.099}_{-0.080}$
Acceptance	0.046	0.011	0.016
Background angular model	0.038	0.017	0.013
Assumption $\delta_S(m_{K\pi}) = \text{constant}$	0.026	0.0048	0.0021
Parameterization of right mass tails	0.036	0.0040	0.0070
Pull bias	—	—	0.0050
TOTAL	0.073	0.021	0.022

Parameter name	$ A_S _{B^0}^2$	$f_L^{B^0}$	$f_{\parallel}^{B^0}$
Value	$0.0371 \pm 0.0099$	$0.5689 \pm 0.0070$	$0.2405 \pm 0.0089$
Acceptance	0.045	0.011	0.016
Assumption $\delta_S(m_{K\pi}) = \text{constant}$	0.026	0.0048	0.0021
TOTAL	0.051	0.012	0.016

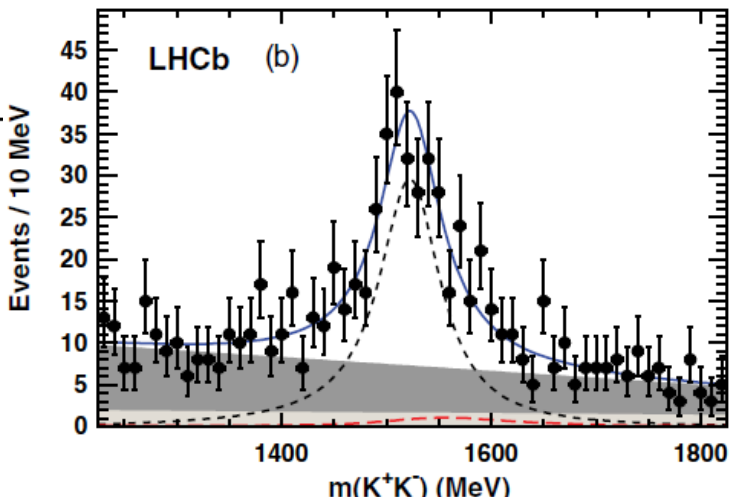
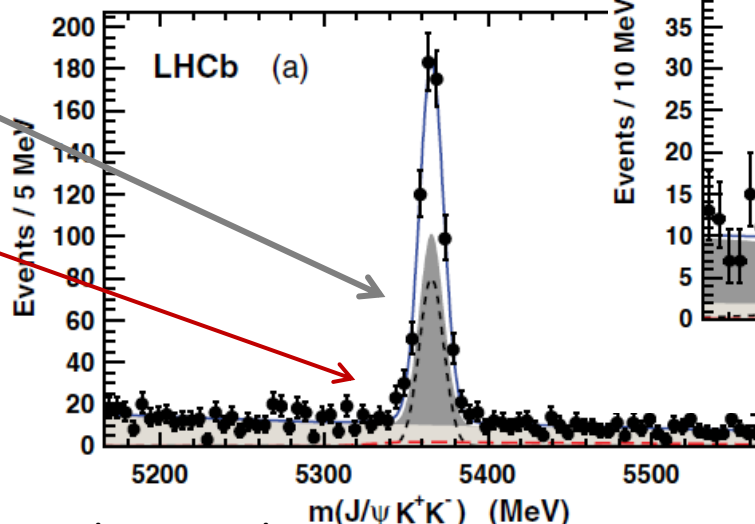


Exploit  $B_s \rightarrow J/\Psi K^+ K^-$  spectrum to find potential channels for  $\phi_s$  measurement

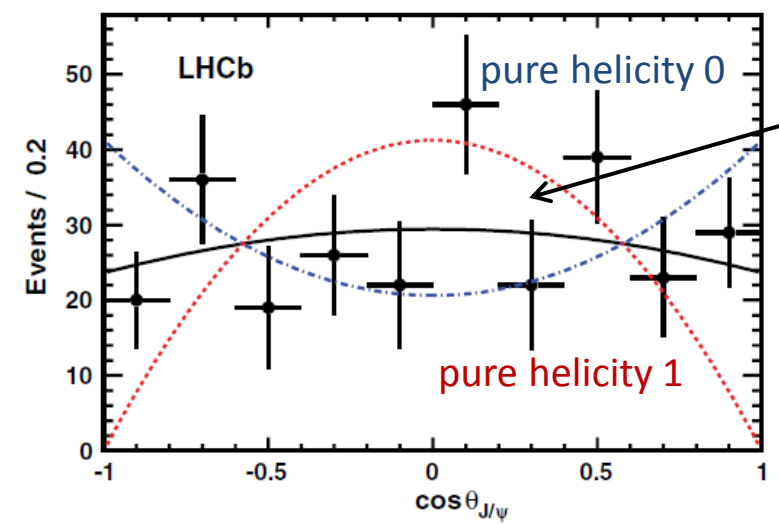
- Simultaneous 2d fit to  $B_s$  and di-kaon mass

accounting for non-resonant  $K^+ K^-$  contribution in the fit

$B_0 \rightarrow J/\Psi K \pi$  reflection bkg



Analyzing  $J/\Psi$  decay angle gives information on spin



consistent with  $f'_2$  contribution

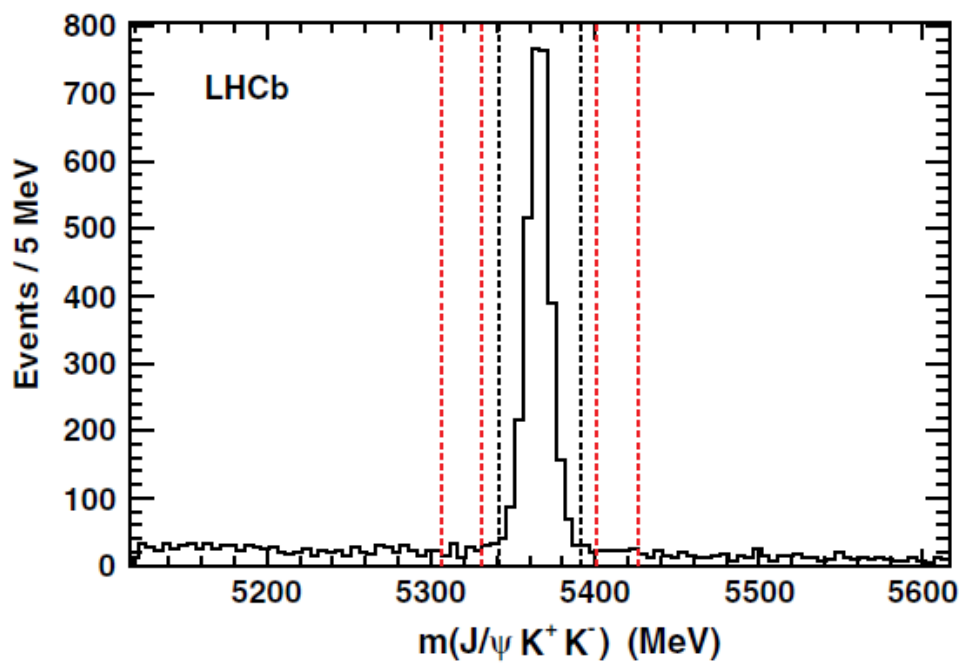
Main systematics:  
 $f'_2$  width, helicity amplitudes

$$\frac{BR(B_s \rightarrow J/\Psi f'_2(1525))}{BR(B_s \rightarrow J/\Psi \Phi)} = (26.4 \pm 2.7 \pm 2.4)\%$$

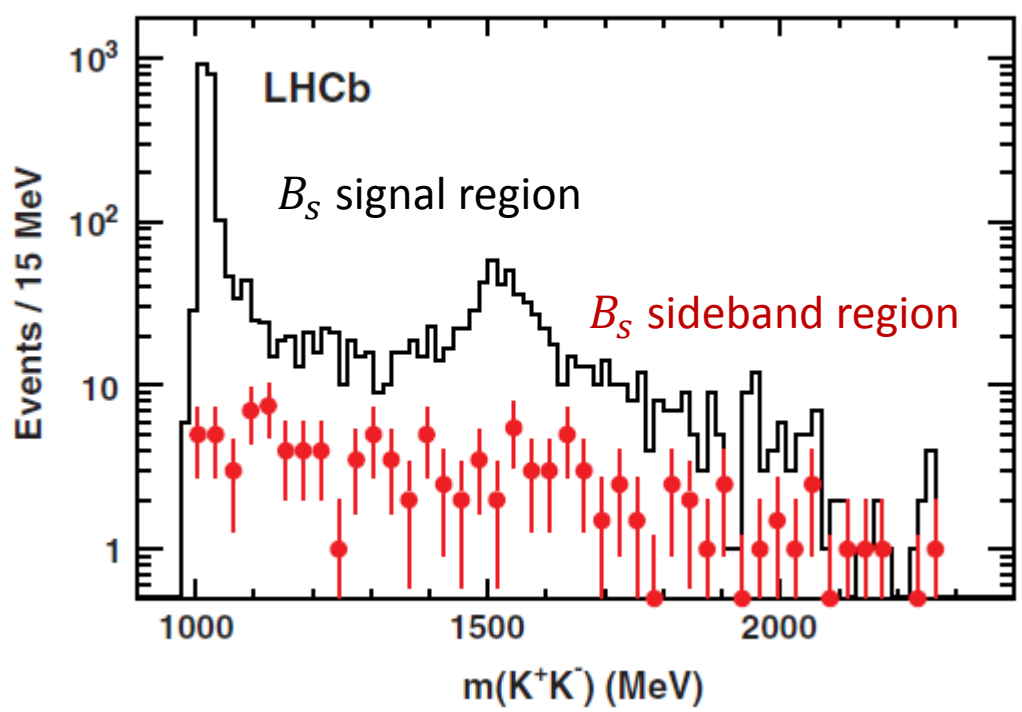
→ first observation of  $B_s \rightarrow J/\Psi f'_2(1525)$  decays



Invariant mass of  $J/\Psi KK$  combinations:



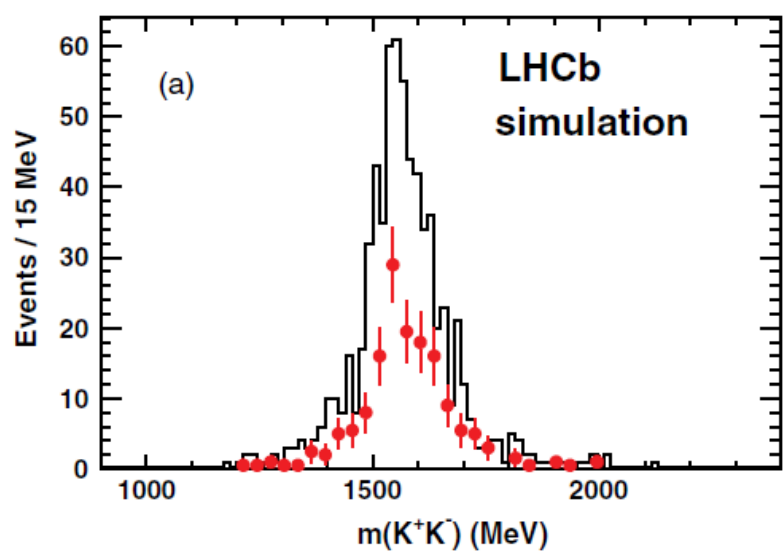
Invariant mass of  $KK$  combinations:



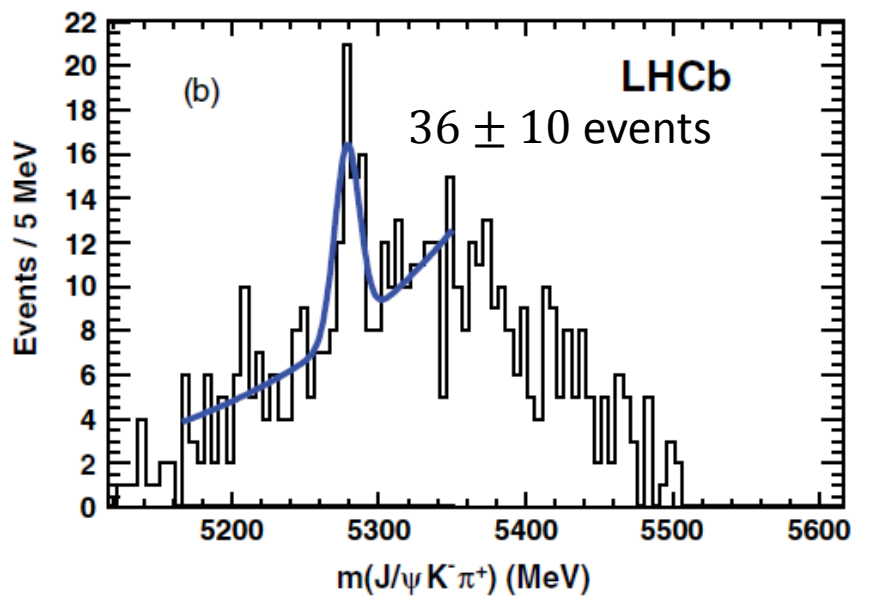


Treatment of  $B_0 \rightarrow J/\Psi K \pi$  reflection background:

Simulated  $B_0 \rightarrow J/\Psi K_2^*$   
with misidentified  $\pi \rightarrow K$



Reconstructed  $J/\Psi KK$  within  
 $[M_{B_S} + 15, M_{B_S} + 200]$  with  $\pi$  hypothesis assigned



→ recalculated to signal region gives  $37 \pm 10$  events  
→ used as constraint in fit to describe reflection bkg.



## Systematic uncertainties:

Source	Change (%)
$f'_2$ width	6.3
Helicity	4.0
Relative efficiency	2.6
$S$ wave under $\phi$	2.3
$K^+ K^-$ mass dependent efficiency	2.3
Background shape	1.3
$\bar{B}_s^0 p_T$ distribution	0.5
$\bar{B}_s^0$ mass resolution	0.5
PID	1.0
Signal shape	1.0
$\mathcal{B}(f'_2(1525) \rightarrow K^+ K^-)$	2.5
$\mathcal{B}(\phi \rightarrow K^+ K^-)$	1.0
Total	9.2

Exotic states  $X(3872)$ 

Eur. Phys. J. C 72 (2012) 1972



- well established exotic state (Belle, CDF, BaBar)

$$B^\pm \rightarrow X(3872)K^\pm, X(3872) \rightarrow J/\Psi \pi^+ \pi^-$$

- popular model:  $D^* \bar{D}$  molecule state  
→ mass should be less than sum of  $D^* \bar{D}$  masses  
 $M_{D^*+D^0} = 3871.79 \pm 0.29 \text{ MeV}/c^2$  (PDG)

Mass measurement at LHCb:

$$m_{X(3872)} = 3871.95 \pm 0.48 \text{ (stat)} \pm 0.12 \text{ (syst)} \text{ MeV}/c^2$$

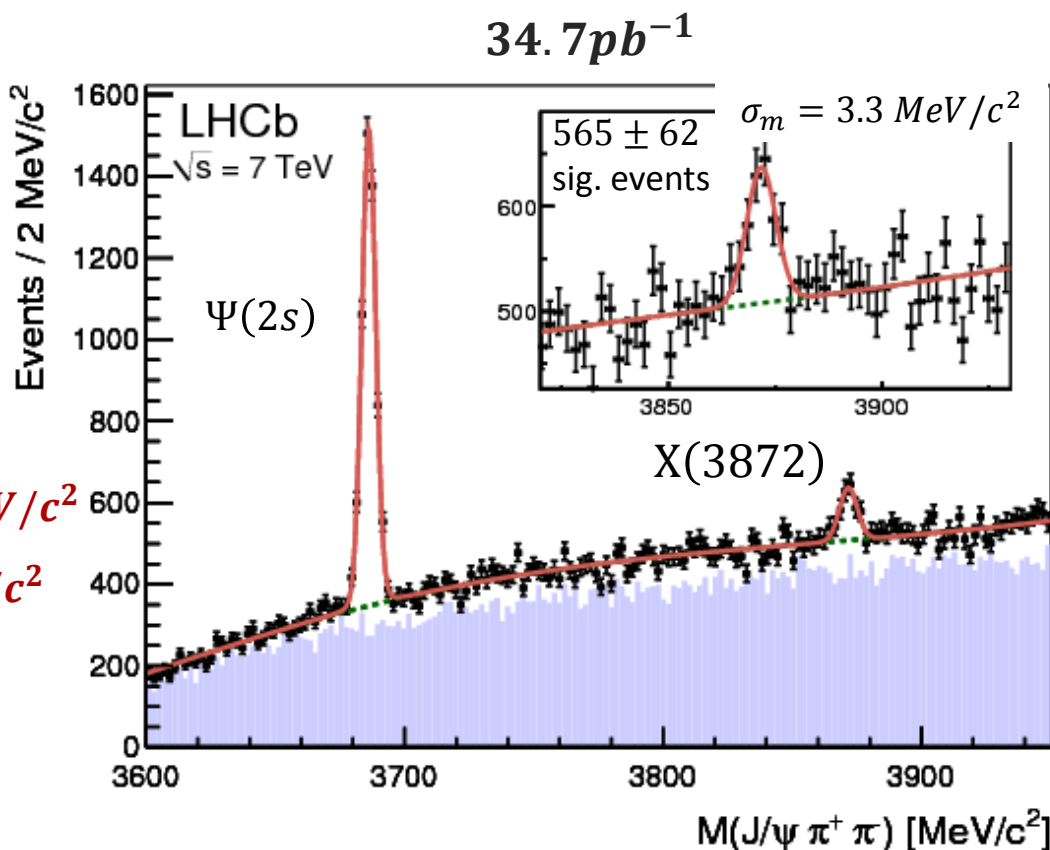
$$m_{\Psi(2s)} = 3686.12 \pm 0.06 \text{ (stat)} \pm 0.10 \text{ (syst)} \text{ MeV}/c^2$$

( $\Psi(2s) \rightarrow J/\Psi \pi\pi$  as control channel)

→ in agreement with PDG and Belle result

**Main systematics:**

momentum scale, energy loss correction



Inclusive production cross section:

(in  $2.5 < \eta < 4.5$ ,  $5 < p_T < 20 \text{ GeV}/c^2$ )

$$\sigma(pp \rightarrow X(3872) + \text{anything}) BR(X(3872) \rightarrow J/\Psi \pi^+ \pi^-) = 5.4 \pm 1.3 \text{ (stat)} \pm 0.8 \text{ (syst)} \text{ nb}$$

2.4 $\sigma$  smaller than predicted for this kinematic region  
(Artoisenet, Braaten, Phys. Rev. D81 (2012) 114018 )

**Main systematics:**  
tracking efficiencies, background model



Systematics uncertainties of mass measurements:

Category	Source of uncertainty	$\Delta m$ [MeV/ $c^2$ ] $\psi(2S)$	$\Delta m$ [MeV/ $c^2$ ] $X(3872)$
Mass fitting	Natural width	–	0.01
	Radiative tail	0.02	0.02
	Resolution	–	0.01
	Background model	0.02	0.02
Momentum calibration	Average momentum scale	0.08	0.10
	$\eta$ dependence of momentum scale	0.02	0.03
Detector description	Energy loss correction	0.05	0.05
Detector alignment	Track slopes	0.01	0.01
Total		0.10	0.12

Systematics uncertainties of cross section measurement:

Source of uncertainty	$\Delta\sigma/\sigma$ [%]
$X(3872)$ polarization	2.1
$X(3872)$ decay model	1.0
$X(3872)$ decay width	5.0
Mass resolution	2.5
Background model	6.4
Tracking efficiency	7.4
Track $\chi^2$ cut	2.0
Vertex $\chi^2$ cut	3.0
Muon trigger efficiency	2.9
Hit-multiplicity cuts	3.0
Muon identification	1.1
Pion identification	4.9
Integrated luminosity	3.5
$J/\psi \rightarrow \mu^+\mu^-$ branching fraction	1.0
Total	14.2



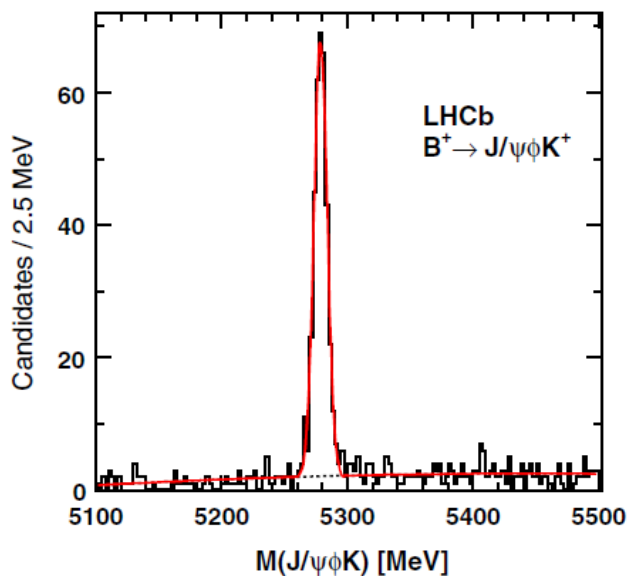
- CDF reported evidence of two exotic states  $X(4140)$ ,  $X(4274)$  (arXiv:1101.6058)

$$B^+ \rightarrow X(4140)K^+, X(4140) \rightarrow J/\Psi \Phi$$

- decay rate to  $J/\Psi \Phi$  should be small and unobservable for charmonia with this mass  $\rightarrow$  exotic

$0.37 fb^{-1}$

LHCb search:  $382 \pm 22$   $B^+ \rightarrow J/\Psi \Phi K^+$  event



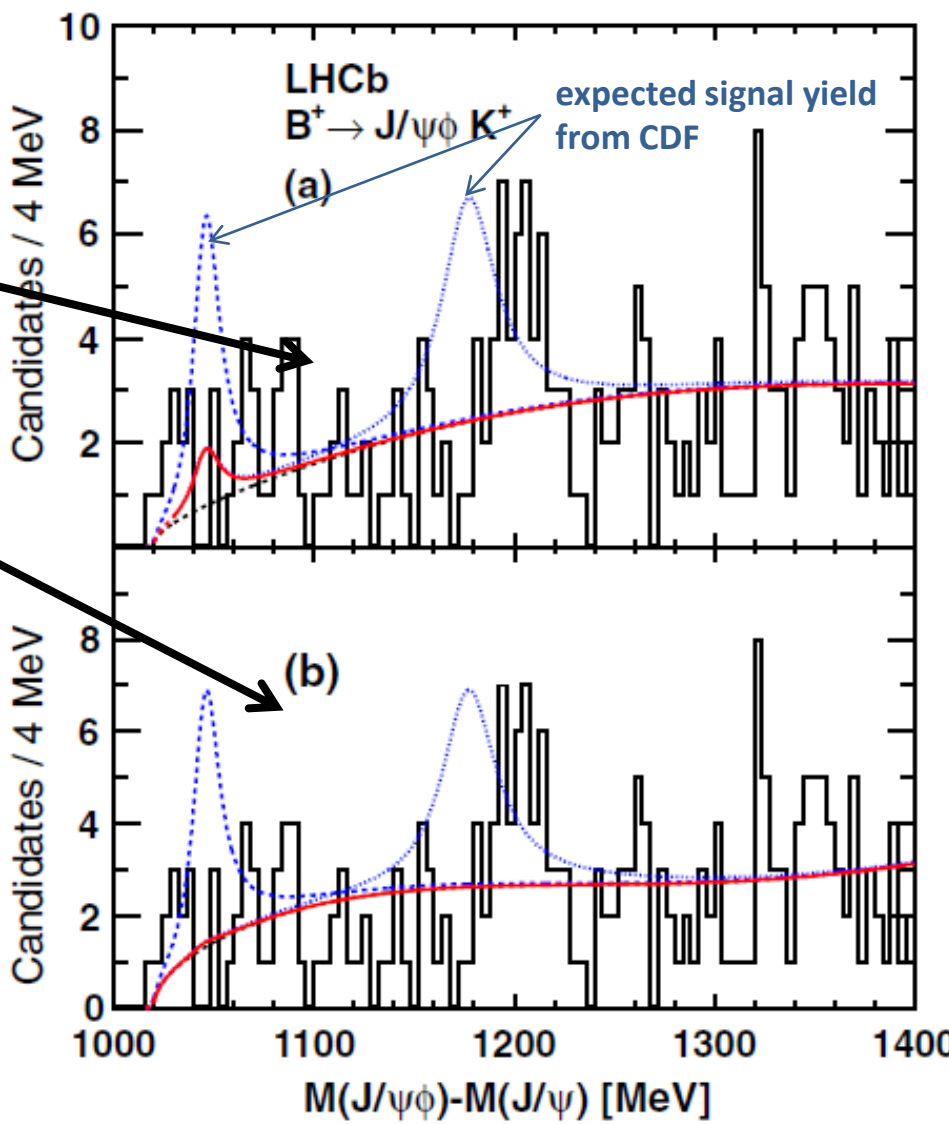
Three-body phase-space background

Three-body phase-space  
Background  $\times$  quadrat. fctn.

$$\frac{BR(B^+ \rightarrow X(4140)K^+, X(4140) \rightarrow J/\Psi \Phi)}{BR(B^+ \rightarrow J/\Psi \Phi K^+)} < 0.07$$

$2.4\sigma$  disagreement with CDF @ 90% C.L.

$$\frac{BR(B^+ \rightarrow X(4274)K^+, X(4274) \rightarrow J/\Psi \Phi)}{BR(B^+ \rightarrow J/\Psi \Phi K^+)} < 0.08$$





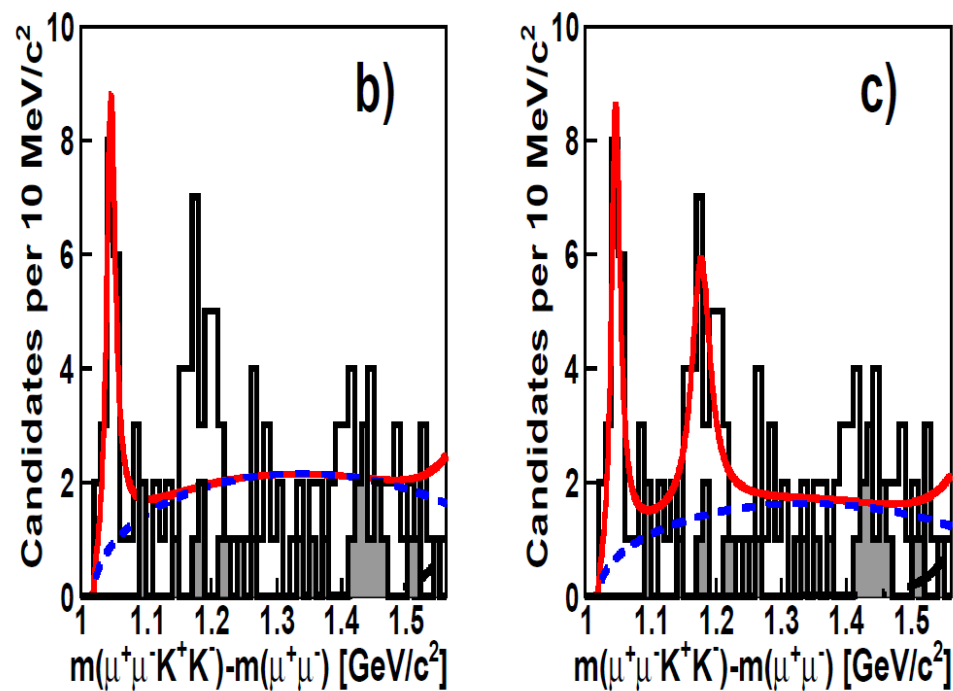
CDF reported evidence of two exotic states  $X(4140)$ ,  $X(4274)$  (arXiv:1101.6058)

Charmonia with this mass can also exploit open flavour decay channels

Decay rate to  $J/\Psi \Phi$  should be small and unobservable (near to kinematic threshold)

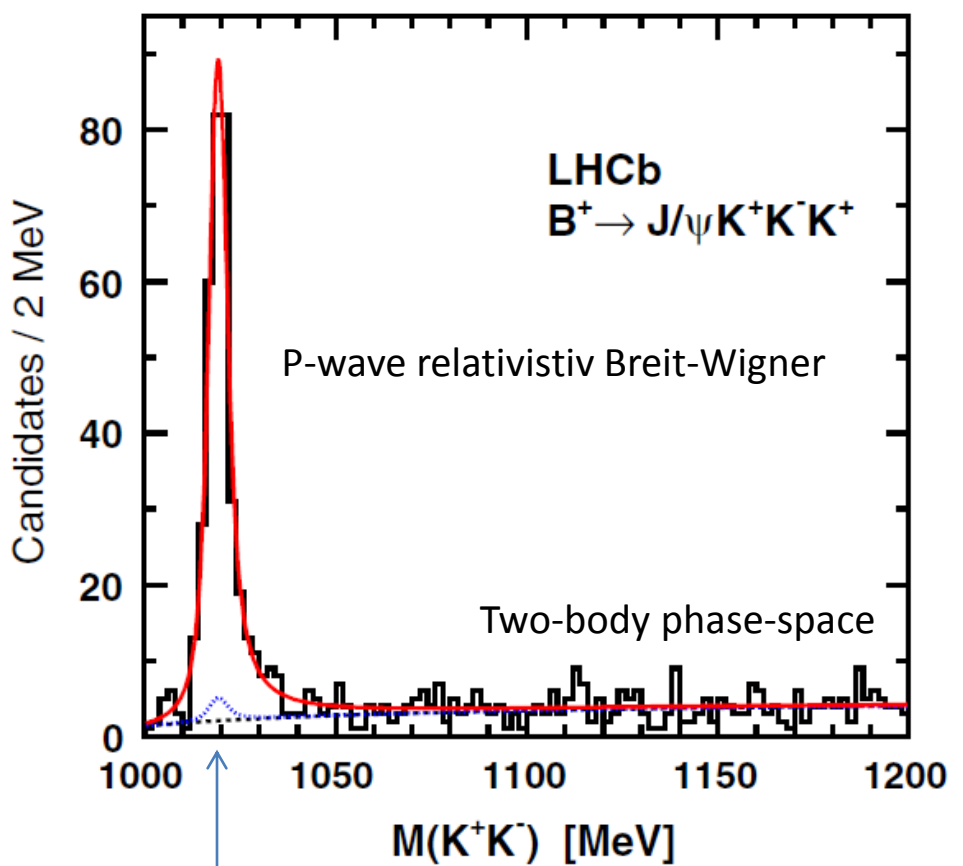
Possible other models: molecular state, tetraquark, hybrid, state, ...

$$\frac{BR(B^+ \rightarrow X(4140)K^+, X(4140) \rightarrow J/\Psi \Phi)}{BR(B^+ \rightarrow J/\Psi \Phi K^+)} = 0.149 \pm 0.039 \pm 0.024$$





$M(KK)$  in  $\pm 2.5\sigma$  region around  $B$ -mass



$14 \pm 3$  bkg events estimated from fit to  $B^+$  mass sidebands

Efficiency correction in  $M(J/\psi \Phi) - M(J/\psi)$  fit

